AD-A235 559

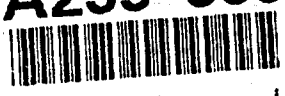

NTATION PAGE

Form Approved
OMB No. 0704-0188

2. REPORT DATE	3. REPORT TYPE AND DATES COVERED
May 1991	Thesis; Aug 89 - May 91

4. TITLE AND SUBTITLE
Target Gas Effects on Collision-Induced Dissociation of Peptides in a Tandem Four-Sector Mass Spectrometer. (U)

5. FUNDING NUMBERS

6. AUTHOR(S)
Captain William Dean Wilson

7. PERFORMING ORGANIZATION NAME(S) AND ADDRESS(ES)
University of Illinois
Urbana, Illinois

8. PERFORMING ORGANIZATION REPORT NUMBER

9. SPONSORING/MONITORING AGENCY NAME(S) AND ADDRESS(ES)
U.S. Army Student Detachment
Ft. Benjamin Harrison, IN

10. SPONSORING/MONITORING AGENCY REPORT NUMBER

11. SUPPLEMENTARY NOTES
Prepared as partial fulfillment of the requirements for Master of Seience in Chemistry under the provisions of AR 621-1, Advanced Civil Scho Schooling Program.

12a. DISTRIBUTION/AVAILABILITY STATEMENT

DISTRIBUTION STATEMENT A
Approved for public release
Distribution Unlimited

12b. DISTRIBUTION CODE

13. ABSTRACT (Maximum 200 words)
The Effects of different target gases on the intensities of the undecapeptide physalaemin during collision-induced dissociation (CID) has been determined to be target mass dependent. The data are consistent to what is predicted by the impulsive theory of energy transfer rather than that of the electronic energy transfer mechanism which is generally accepted.

14. SUBJECT TERMS Mass Spectrometry, Tandem, Collisional Dissociation, CID, Four-sector

15. NUMBER OF PAGES

16. PRICE CODE

17. SECURITY CLASSIFICATION OF REPORT	18. SECURITY CLASSIFICATION OF THIS PAGE	19. SECURITY CLASSIFICATION OF ABSTRACT	20. LIMITATION OF ABSTRACT
Unclass	Unclass	Unclass	

TARGET GAS EFFECTS ON COLLISION-INDUCED DISSOCIATION OF PEPTIDES IN A TANDEM FOUR-SECTOR MASS SPECTROMETER

BY

WILLIAM DEAN WILSON

B.S., The University of Alabama, 1980

THESIS

Submitted in partial fulfillment of the requirements
for the degree of Master of Science in Chemistry
in the Graduate College of the
University of Illinois at Urbana-Champaign, 1991

Urbana, Illinois

UNIVERSITY OF ILLINOIS AT URBANA-CHAMPAIGN

THE GRADUATE COLLEGE

MAY 1991

WE HEREBY RECOMMEND THAT THE THESIS BY

WILLIAM DEAN WILSON

ENTITLED TARGET GAS EFFECTS ON COLLISION-INDUCED DISSOCIATION OF PEPTIDES IN A TANDEM FOUR-SECTOR MASS SPECTROMETER

BE ACCEPTED IN PARTIAL FULFILLMENT OF THE REQUIREMENTS FOR THE DEGREE OF MASTER OF SCIENCE

Director of Thesis Research

Head of Department

Committee on Final Examination†

Chairperson

† Required for doctor's degree but not for master's.

ABSTRACT

The effect of different target gases on the intensities of the daughter ions of the undecapeptide physalaemin during collision-induced dissociation (CID) has been determined to be target mass dependent. The FABMS/MS spectra showed primarily higher mass fragments for lower mass target gases and lower mass fragments for higher mass targets. The data are consistent with what is predicted by the impulsive theory of energy transfer. The daughter ion intensity difference can be explained by energy transfer efficiencies approaching a maximum as the average atomic mass of the target approaches that of the parent ion. The decreasing intensity of higher mass daughter ions can be explained by sequential fragmentation from higher mass daughter ions to low mass daughter ions, an energy dependent process.

Dedication

To my darling wife Susan and to my three wonderful sons, who have given up their husband and father during this arduous process. Thank you for your love, support, and patience.

Acknowledgements.

This work was possible through the funding of the National Institute of General Medical Sciences (GM 27029) and the University of Illinois's University Scholars Program. The U. S. Army Advanced Civil Schooling Program provided for coursework and thesis preparation expenses. I would also like to thank the members of the Rinehart research group for their assistance and useful comments throughout and, in particular, Mark Proefke and Nancy Fregeau for their extremely helpful comments and critiques. I would like to thank Dr. Richard Milberg, Director of the Mass Spectrometry Laboratory, and the rest of his staff for their training support, assistance, and patience during my research. Finally, I want to thank Professor Kenneth L. Rinehart, my research advisor, for his invaluable guidance, direction, and support throughout this effort.

I. Introduction.

In mass spectrometry, sample molecules are ionized and then separated by their mass-to-charge ratio prior to detection. Unique structural information about a molecule can be then inferred from the ion and its fragments. The sensitivity of this technique is truly outstanding with usable spectra obtainable from as little as 10^{-14} g of sample.[1]

Despite its great value, problems do occur, especially for larger mass molecules such as peptides. Often large peptides do not produce molecular ions or undergo useful fragmentation due to the ability of the molecule to disperse extra energy from ionization throughout the molecule. Another problem is that "soft" ionization techniques, such as fast atom bombardment, (FAB) often give stronger molecular ions but chemical noise such as matrix ions can confuse the spectrum. The problem of purification of peptides also can cause difficulty since a reasonably pure sample is needed for a conventional mass spectrum.[2]

By replacing the detector of a conventional mass spectrometer with a second mass spectrometer (thereby placing the two "in tandem") with an activation region between them, a selected ion can be induced to fragment further and the spectrum of that fragmentation obtained. Many of the problems associated with conventional mass spectrometry are thereby reduced.[1]

A. Tandem Mass Spectrometry Theory.

The theory behind tandem mass spectroscopy (MS/MS) is simply that an ion produced and separated in one mass spectrometer can be focused into an activation region where it can gain sufficient energy to induce unimolecular decomposition. After fragmentation, the fragment ions can be further analyzed by a second mass spectrometer. This can be shown in "Black Box" fashion in Figure 1. As shown, any combination of ion sources and mass-to-charge ratio analyzers can be used to introduce the ion of interest into the activation region and in practice almost all methods have been tried.[1,3]

In the activation region, the ion is imparted with sufficient activation energy to undergo spontaneous unimolecular dissociation. Energy is transferred to the parent ion by one or more of the following methods: collisional activation, photodissociation, electron excitation, and suface-induced dissociation. I shall discuss each of these techniques later in this introduction.

The second mass spectrometer takes the fragments produced in the activation region and analyzes them by their mass-to-charge ratios. This analysis may be performed by magnetic and/or electric sectors, quadrupole mass analyzers, time-of-flight, ion trap, and Fourier transform-ion cyclotron resonance instruments. I shall also briefly discuss the theory of operation of each of these instruments later in this introduction.

B. Activation Reactions.

Once the ion of interest has been selected by the first mass spectrometer, it is introduced into an activation region to obtain enough energy to cause unimolecular dissociation. This can be described by the following mechanism:[4]

$$P^+ + M \longrightarrow [P^+]^* \qquad (1)$$

$$[P^+]^* \longrightarrow d^+ + n \qquad (2)$$

Where: P^+ is the parent ion selected.
$[P^+]^*$ is the "energized" or "activated" parent ion.
d^+ is the daughter ion produced from fragmentation.
n is the neutral fragment lost.
M is the activating species.

The term "parent ion" is used here since any ion in the normal mass spectrum can theoretically be selected as a parent ion although often the molecular ion is selected. The power of this technique comes partly by this ability to select any ion one wishes and obtaining a fragmentation spectrum of it.

Many variations of activating species have been tried, from gas molecules (collisional activation) to photons, electrons, and even surfaces.

1. Collisional Activation.

(a) Theory.

The most accepted theory of unimolecular dissociation, the Quasi-Equilibrium Theory (QET), recognizes that in collisional induced dissociation (CID), the collision causes excitation but the excitation can be electronic, vibrational, or rotational or a combination of these. It also requires that for electronic excitation, the energy must first be converted to vibrational modes because the dissociation process is known to be from the ground electronic state.[4] The energy is then rapidly randomized through the molecule in the case of a polyatomic parent ion. Under QET, the molecule doesn't remember how it became excited. When localization of vibrational quanta occurs at weaker bonds in excess of the dissociation energy, the bond breaks resulting in daughter ions.[4]

(b) Energy Transfer Mechanism.

The mechanism of energy transfer and internalization in collisions is in debate. The traditional explanation is that it occurs primarily through electronic excitation during the collision. The other explanation is that the excitation is impulsive and is a result of momentum transfer between the target and parent ion.[5]

(1) Electronic Excitation.

When the parent ion approaches the target gas, the Coulombic forces between the charged particles begin to interact. If we assume that charged particles of the target gas are stationary in the timeframe of the collision, then the energy transfer for each electron-electron interaction is given by[6]

$$\Delta E(b) = \frac{2(ze^2)^2}{mv^2}\left(\frac{1}{b^2}\right) \quad (3)$$

Where $\Delta E(b)$ = energy transferred.

e = elemental charge.

m = mass of an electron.

b = interaction distance.

v = velocity of the charged particle.

z = number of charges involved.

The energy transferred is the momemtum imparted to the charged particles in the direction transverse to the path of the moving particle (parent ion in our case).

As this equation predicts, the energy is dependent on the proximity of the interaction, the velocity of the ion, and its charge. In a collision between an ion and a neutral target gas, the energy imparted is the sum of the interactions between all nuclei and electrons. If the velocity of the parent ion is sufficently fast then this equation is valid and energy transfer

occurs. What is generally observed is that the energy transferred places the electrons of the parent ion into an excited electronic state. This electronic excitation mechanism can be explained by non-adiabatic curve crossing between the ground electronic state and the first excited electronic state of the parent ion at the instant of excitation. Figure 2 shows graphically how this curve crossing occurs. As the two colliding species approach each other, the electron orbitals begin to interact and the Coulombic interaction causes deformations to occur. These deformations increase the potential energies of the orbitals. The separation between the "ground state" and "excited state" becomes smaller, as represented by the two curves in part (a) of the diagram. As part (a) shows, if the collision is slow enough the electron orbitals adjust to keep the lowest total potential energy. This is an adiabatic interaction and no crossing is observed between the states. Any energy transferred is simply translational energy and is observed as scattering. If as shown in part (b), the interaction is fast enough that the orbitals cannot adjust adiabatically in time, the possibility exists that the curves will cross. In this type of interaction, the parent ion would be left in an excited electronic state after the collision.

The probability function for this type of curve crossing excitation has been estimated by McLafferty[7] to be approximately Gaussian in shape. The maxima of this probability function will occur at a point where the Massey criterion (given by the following equation) is valid:[8]

$$v = \frac{\delta E a_e}{h} \qquad (4)$$

Where: δE is the energy separation of the ground and excited states at the moment of impact.

a_e is the interaction distance (which is on the same scale as Lennard-Jones diameters)

h is Planck's constant.

v is the velocity of the parent ion.

The amount of energy transferred during this process is then ΔE, the difference between the ground and excited electronic states shown in Figure 2 (ca. 6 eV and not δE in equation 4). The Massey criterion equation (Eq. 4) is not a measure of the energy transferred in the collision but rather the relationship between the energy separation between electronic states and the velocity of the moving ion. This equation assumes that the interaction distance, a_e, is a constant for all systems but this is not strictly true and is approximately the combination of the Lennard-Jones diameters of the target and parent ion.[8] If this interaction distance increases but parent ion velocity remains constant, the equation predicts the maximum to also move to lower δE. This shift means that adiabatic interaction is more likely to occur. The argument then is that as parent ion mass increases the amount of energy transferred by this mechanism becomes less probable.

(2) Impulsive Excitation.

Another theory suggests that the interaction is impulsive and the energy is directly deposited into vibrational or rotational states through atom-atom interactions during the parent ion-target gas collision. The energy then is randomized and dissociation occurs when sufficient quanta localize in "weak" bonds.[3]

In this technique of energy transfer, an ion moving at a given velocity has kinetic energy, $mv^2/2$, and momentum, mv. If the ion collides with another gas molecule, part of the kinetic energy of the two can be converted into internal energy of one or both of the collisional partners. The equations for conservation of momentum and energy for this event, assuming a "hard sphere" elastic (no energy lost) collision occurring in one dimension are:

$$m_p v_{pi} + m_t v_{ti} = m_p v_{pf} + m_t v_{tf} \quad (5)$$

$$m_p v_{pi}^2 + m_t v_{ti}^2 = m_p v_{pf}^2 + m_t v_{tf}^2 \quad (6)$$

where m_p = mass of the parent ion.

m_t = mass of target gas molecule.

v_{pi}= initial velocity of parent ion.

v_{ti}= initial velocity of target gas molecule.

v_{pf}= final velocity of parent ion.

v_{tf}= final velocity of target gas molecule.

Solving equation (5) for v_{tf} we get

$$v_{tf} = v_{ti} + (m_p/m_t)(v_{pi} - v_{pf}) \tag{7}$$

and if we insert this into equation (6):

$$m_p(v_{pf}^2-v_{pi}^2) + 2m_p(v_{pi}-v_{pf})v_{ti} + (m_p^2/m_t)(v_{pi}-v_{pf})^2 = 0. \tag{8}$$

Because of the conservation laws of energy and momentum, the initial velocities must also satisfy equation (8), so then we can divide by $(v_{pf} - v_{pi})$. After we do this we get:

$$m_p(v_{pf} + v_{pi}) - 2m_pv_{ti} + (m_p^2/m_t)(v_{pf} - v_{pi}) = 0 \tag{9}$$

or

$$v_{pf} = [2m_tv_{ti} - (m_t - m_p)v_{pi}]/(m_p + m_t) \tag{10}$$

What this equation describes is how the velocities change during a one dimensional collision. The velocities before and after collision are determined by the ratio of the masses of the two colliding species. If $m_p = m_t$, then $v_{pf} = v_{ti}$ and from equation (5) then $v_{tf} = v_{pi}$. This simply means that the velocities are exchanged during the collision. In actual collisions between atoms and molecules, the collision is

inelastic and some of the energy is transferred from translational to internal energy of one or both of the atoms or molecules. The maximum amount of energy available is given by the translational energy of the parent ion and the temperature of the target gas. The amount of that energy transferred to internal modes can be given by

$$Q = \varepsilon E_{total} \tag{11}$$

where Q = amount of energy transferred to internal modes.

E_{total}= total energy of the two atoms or molecules.

ε = energy transfer coefficient.

The energy transfer coefficient, ε, from an inelastic collision between two particles of differing masses can be determined by deriving the transfer coefficient of the system at the low temperature limit (0°K) where the only energy would be the translational energy of the parent ion. Since v_{ti} is zero here, then equations (6) and (9) become:

$$v_{pf} = (m_p - m_t)v_{pi}/(m_p + m_t) \tag{12}$$

and:

$$m_p v_{pi}^2/2 = m_p v_{pf}^2/2 + m_t v_{tf}^2/2 + \Gamma \tag{13}$$

The amount of energy internalized, Γ, is proportional to the amount of energy available so this can be expressed as:

$$\Gamma = \chi(m_p v_{pi}^2/2) \tag{14}$$

Where χ = energy transfer efficiency factor.

The maximum energy internalization would occur in two limiting cases, the first is when the parent ion and the target gas are at rest after collision and all the translational energy is internalized. This is the ideal inelastic collision and is never realized in practice and is neglected in our discussion. The other limiting case is where the target remains at rest after collision ($v_{tf} = 0$) so that all translational energy lost by the parent ion is internalized, then:

$$m_p v_{pi}^2/2 = m_p v_{pf}^2/2 + m_t v_{tf}^2/2 + \chi(m_p v_{pi}^2/2) \tag{15}$$

and if v_{pf} is replaced by equation 12 and we solve for χ, we get (after a little algebra),

$$\chi = 4m_p m_t/(m_p + m_t)^2 \tag{16}$$

It can be shown[9] that going to 3 dimensions causes equation (11) to change to:

$$Q = \chi E_{cm}/2 \tag{17}$$

and then

$$\chi/2 = \varepsilon \tag{18}$$

This internal energy, Q, can then be localized into various bond vibrational modes. If sufficient quanta of energy are localized in a given bond so that the energy is greater than the dissociation energy for that bond, cleavage will occur.

Derrick has modified this theory by looking at the nuclear

"knock-on" event from a statistical standpoint.[10] If the collision occurs mainly between an atom of the parent ion and target gas, then the "best" energy transfer predicted by the impulsive theory occurs when the two atoms are the same mass. In this case ($m_p = m_t$) and equation (16) reduces to one. The average amount of energy that is transferred is then determined statistically as the probability of the target atom colliding with any given atom of the parent ion. The general method for calculating these statistical atomic weights is given by equation (19) below.

$$\sum P(A) * A = M_{stat} \qquad (19)$$

Where $P(A)$ = Probability of target colliding with atom A of the parent ion.

A = Mass of atom A.

M_{stat} = Parent ion statistical mass.

If one assumes the probability of collision is the same for each atom in the parent ion and target gas, then the average atomic mass of the parent ion and target gas can be used in the impulsive theory equations. Various calculated average masses for types of compounds are given in Table I.

(c) Competing Processes

Complications arise in collisional activation that degrade the utility of this method. When the parent ion and target gas collide, more things can happen than a direct "head-

on" inelastic collision resulting in collisional activation.[11] Some of these are scattering of the parent ion beam, neutralization of the parent ion, charge exchange between the parent ion and target. These processes also are the result of collisions between the parent ion and target gas. The result is a competion occurring between these processes in a given collision pair under one set of conditions. How these competing processes relate to the same factors as collisional activation and their impact on the CID process will be briefly discussed.

(1) Scattering.

Here the target and ion collide in such a manner that the ion is deflected from its trajectory to a degree that the ion optics of the mass spectrometer cannot collect and focus it. It has been reported[10] that the cross section for scattering, σ_s, is based on the equation for an atomic ion-atomic target collision formula,

$$\sigma_s \approx (a_e/v)^2 \qquad (20)$$

where a_e = distance at which the target and ion interact.

v = velocity of the ion

This equation predicts that as the interaction distance increases and the velocity of the parent ion decreases, the scattering cross section increases rapidly. Thus if the parent ion remains at the same accelerating potential and the targets

are changed, scattering will also increase as the square of the interaction distance (roughly proportional to the molecular weight of the target).

(2) Charge Exchange.

The ion can be neutralized by capturing an electron from the target gas. For charge exchange the cross section, σ_n, is to a first approximation inversely proportional to the difference between the ionization energies of the target and the ion.

$$\sigma_n \approx 1/|D_{o(pi)} - D_{o(t)}| \qquad (21)$$

Where $D_{o(pi)}$ = Ionization potential of the parent ion.

$D_{o(t)}$ = Ionization potential of the target gas.

(3) Charge Stripping, Charge Inversion, or Target Gas Activation.

In charge stripping, the target gas removes another electron from the parent ion, resulting in a doubly-charged ion. Charge inversion occurs when the target donates two electrons to the ion resulting in a negative parent ion. Target gas activation is when the target gas internalizes some or all of the translational energy lost as a result of the collision. The cross sections of these competing processes are generally considered to be small in relation to the others.

These processes together reduce the parent ion intensity as a function of parent ion mass. Ionization intensity from the first mass spectrometer also decreases with increasing mass of the sample molecule. With these two factors in mind, tandem mass spectrometry of high mass samples (>1500 daltons) using collisional activation is difficult. In addition, the requirement to use gas pressures of ca. 1 torr in the collision cell require a large differential vacuum pumping requirement, thereby increasing the cost of the instrumentation.

2. Photodissociation.

This technique uses absorbed photons as its source of activation energy. The parent ion beam is intersected with a beam of light whose wavelength is selected as being capable of absorption by the ion. The low cross section for this event ($\sim 10^{-2}$ Å^2)[3] requires high intensity sources of monochromatic light (lasers) and a slow ion or multiple path system to increase the probability of absorption of a photon by each ion. As a result most of the early work was done on Fourier Transform - Ion Cyclotron Resonance (FT-ICR) and triple quadrupole instruments but recently sector instruments have been used[3]. Ion trap instruments show great promise in this type of activation method since they can store ions for relatively long periods of time like ICR instruments.

The low fragmentation yield for this process in beam instruments is evidenced by the shift of research into using

tunable lasers to give a daughter ion spectrum as a function of wavelength.[3] This gives a method of identifying isomeric ions, since the total ion current vs wavelength (corrected for metastable and residual gas collisionally activated fragmentation) is almost a fingerprint for a particular ion. This spectrum is similar to an absorption spectrum but only relaxations by photon-induced dissociations are recorded and other events (e.g. fluorescence) are not.

3. Electron-Induced Dissociation.

This method uses a beam of electrons somewhat lower in energy than that used for electron impact ionization (≤40 eV generally) to bombard the parent ions in the activation region. Initial experiments by Freiser, et al., were with an FT-ICR instrument,[12-15] but EID has also been performed in sector instruments.[16] The mechanism of excitation with electron bombardment appears to be of the Franck-Condon type (vertical electronic transitions). This would be caused by the interaction of the ion's molecular orbitals with the rapidly changing electric field generated by the fast moving electron as it passes near or through the polyatomic parent ion. This effect would be similar to white light irradiation but with optically forbidden transitions available.

This technique has similar advantages to that which photodissociation has over collisional activation: lower vacuum pumping requirements, reduced scattering of the parent ion, and

no charge transfer reactions with a target gas. The cross section for electron induced dissociation is larger than photodissociation and the instrumentation is less expensive and complex. The required flux and electron energies are easier to achieve and more variable than can be done with photons. Still, this technique will need more research to determine if this technique could rival collisional activation in effectiveness.

4. Surface-Induced Dissociation.

This method of activation simply involves crashing the parent ion into a solid surface thereby imparting enough energy to cause the ion to fragment.[3] The basic energy transfer mechanism is thought to be the same as in collisional activation but with a more narrow band due to the lack of translational motion of the target molecules. The geometry of the instrument must be "bent" in beam instruments to allow focusing of the ions after a glancing impact on the surface.[15] The use of microchannel plates can alter this restriction. The major limitation is in the charge neutralization that can occur. This is thought to be the major competing process so that only 0.5% of the ions are successfully detected after the collisional event.[3]

C. Mass-to-Charge Ratio Analysis.

Many different instruments exist to separate and select the parent ion, then collect and analyze the daughter ions[3]. In tandem mass spectrometry, the fragmentation of parent ions causes daughter ions to have different momenta and kinetic energies due to the loss of the neutral fragment mass. Because of this fact, we must discuss the processes by which various instruments select daughter ions for detection.

1. Sector Instruments.

Sector instruments are ideally suited for MS/MS analysis in that they can select the parent ion with high resolution for introduction into the activation region and subsequent analysis. The analysis of the daughter ions can also be performed with similar resolution if a second double-focusing instrument is used. Mass analysis in sector instruments occurs by use of an electric sector, magnetic sector, or both as in the high resolution double focusing design.

(a) Electric Sector.

This sector selects ions based on their kinetic energy to charge ratio. The principle is best shown by the equation of motion of a moving ion is an electric field shown below: [17]

$$\frac{mv^2}{r} = zE \tag{22}$$

The kinetic energy of the parent ion departing the ion source is given by

$$mv^2/2 = zV \tag{23}$$

where m = mass of the ion (kg)

v = velocity of the ion (m/s)

r = radius of deflection

z = charge on the ion (Coulombs)

E = electric field strength (Volts/m)

V = accelerating voltage of ion source

so by combining equations (22) and (23) we get

$$\frac{mv^2}{z} = Er = 2V \tag{24}$$

Since both E and V are constant , the sector will only allow ions with the given kinetic energy-to-charge ratio to pass. If the ion fragments after it has been accelerated, then the kinetic energy of these daughter ions changes due to changes in their mass (velocity remains constant). If the parent ion mass is known then the daughter ions can be collected by changing the electric field by use of the following equation:

$$\frac{E_p m_d z_p}{m_p z_d} = E_d \tag{25}$$

Where E_p = electric field strength required to pass the parent ion.

m_p = mass of parent ion.

m_d = mass of daughter ion.

z_p = charge on the parent ion.

z_d = charge on the daughter ion.

(b) Magnetic Sector.

This sector separates ions based on their momentum-to-charge ratio because of the effect of the magnetic field on the path of the ion. The motion of the ion is given by[17]

$$\frac{mv^2}{r} = zvB \tag{26}$$

or

$$\frac{mv}{z} = Br = 2V \tag{27}$$

using the same argument as in the electric sector, where B is magnetic field strength and the other terms are as previously described.

As we can see here also, if magnetic field strength and accelerating voltage are constant then only ions with the appropriate momentum-to-charge ratio are collected.

(c) Double Focusing.

In a double focusing instrument, the electric sector (E) and magnetic sector (B) previously described are connected together in either combination. The advantage gained is that by selecting a given kinetic energy by holding the electric field constant, the magnetic field can be scanned to separate the ions based on mass-to-charge ratio as shown in the following equation:[17]

$$\frac{m}{z} = \frac{(Br)^2}{2V} \tag{28}$$

Sector instruments generally operate with constant accelerating voltages of several thousand volts. As a result of these high energies, the activation method most often used for MS/MS in these instruments is collisional activation with an appropriate target gas, usually helium.

2. Quadrupole Instruments.

In contrast to sector instruments, these instruments have ion kinetic energies of only a few to tens of volts. These slow ions are passed through a region where they are subjected to a dc voltage (V_1) and an rf voltage ($V_o \cos t$; t is time) from rods that are hyperbolic. The equations of force for the ions are:[3]

$$F_y = ma_y = \mathbf{z}(V_1 + V_o\cos t)(2y/r_o^2) \quad (29)$$

$$F_z = ma_z = -\mathbf{z}(V_1 + V_o\cos t)(2z/r_o^2) \quad (30)$$

$$F_x = ma_x = 0 \quad (31)$$

where **z** is the number of charges on the ion.

y is the y coordinate position.

z is the z coordinate position.

m is the mass of the ion.

$a_{x,y,or\ z}$ is the acceleration along that coordinate axis.

Here the x axis is the axis of the instrument and r_o is the largest circle that can be inscribed inside the rods of the quadrupole. The ions move in a complicated path through the instrument but for any given combination of accelerating voltage, dc voltage, and rf voltage only one mass-to-charge combination will reach the detector.

Quadrupole instruments are advantageous in tandem mass spectrometry due to their lower cost and smaller size. In addition, the lower translational energy of the parent ion eases use of other activation methods such as photodissociation, EID, and SID. In addition, the fragmentation patterns from collisional activation reflect the lower energies of the collisional interaction.

3. Time of Flight.

This instrument operates in a pulsed mode where a packet of ions is formed, accelerated by an applied voltage and separated by their flight times down a drift tube to a detector. The formula for equating mass/charge to flight time (T) is[17]

$$T = L\left(\frac{m}{2zV}\right)^{1/2} \tag{32}$$

Where L = length of ion path

V = Accelerating voltage

Although useful in pulsed ionization techniques, this instrument requires precise timing electronics coupled with a reflection grid to separate the parent ions in tandem mass spectrometry applications.

4. Fourier-Transform/Ion Cyclotron Resonance.

This instrument is based on the ion cyclotron resonance phenomenon where an ion moves in a circular orbit described by the formula:[17]

$$\omega_c = \frac{zeB}{2\pi m} \tag{33}$$

Where ω_c is the cyclotron frequency of the ion.

e is the charge of an electron.

In the FT-ICR experiment, ions are formed and then an electromagnetic frequency band pulse (chirp) is applied to a square cell containing the ions under high vacuum (10^{-9} torr) in a very strong magnetic field. The ions will move coherently with the excitation pulse. Receiver plates on the cell are induced by the movement of the ions to generate a current that matches the cyclotron frequencies of the ions. This complex signal is deconvoluted by Fourier transform analysis to yield a mass spectrum. The advantage of this technique is that ion lifetimes are long and multiple experiments can be averaged. In tandem mass spectrometry, the ions can be activated to fragment by any of the activation methods previously described and fragments analyzed in the same cell. Collisional activation is more difficult due to high vacuum requirements, but daughter ion spectra can be generated for all the ions generated in the original ionization.

5. Ion Trap.

The ion trap is a three dimensional quadrupole and similar equations for ion motion apply. The ion trap functions like the ICR instrument in that the ions are "trapped" in the cell by a low rf frequency. The spectrum is obtained by increasing the rf frequency which causes ions of higher and higher masses to be ejected and thereby detected. One major

difference in an ion trap is that a "bath gas", of helium usually, is maintained at pressures of about 10^{-3} torr to stabilize the ion through its damping effect. This damping effect is decribed as the loss of translational motion of the ions which force the ions back toward the center of the ion trap. This increases both resolution and sensitivity. This bath gas (which can be the target gas for CID as well) and ion storage capability makes ion trap instruments well suited for MS/MS experiments.[3]

II. Experimental

A. Apparatus.

1. Mass Spectrometer.

A VG Analytical 70-SE4F tandem double-focusing mass spectrometer of EBEB geometry was used for all experiments.[18] Ions were formed by a fast atom bombardment source with a Xe gun set at 8 KeV with a current setting of 1.2 mA. The instrument's resolution was set at 1000 for both halves of the instrument. The cell was floated at 1/2 the accelerating voltage (source acceleration at 8 KeV, collision cell "floated" at 4 KeV) for all experiments to optimize transmission and fragmentation. The second half was calibrated using a calibration-only FAB source just prior to the collision cell and a calibration salt mixture described elsewhere.[18]

The target gases/vapors were introduced by one of two inlet systems described below via a capillary into a 2-cm path length aluminum collision cell. The attenuation for the parent ion beam was set at 90 per cent for all experiments. The data were collected using a VG 11-250J data system in MCA mode. Each experiment consisted of 2 scans (averaged by the data system) per run and at least 3 runs per experiment (which were then measured and averaged manually).

2. Target Gas/Vapor Inlet System.

The target gas or vapor was introduced by one of two inlet systems based on whether the target was a gas or liquid at room temperature.

a. Gases.

For gases the inlet system was simply a supply tank of the desired gas regulated at 20 psi and connected to a T joint as shown in Figure 3a. The other two sides of the T connector were for a roughing vacuum pump and for the inlet capillary to the collision cell. The flow of gas into the cell was metered through the existing metering valve for the instrument. The transfer line from the supply tank regulator to the metering valve at the collision cell was thoroughly evacuated and then purged three times before each experiment by introducing small amounts of the target gas into the line and then evacuating the

line again.

b. Vapors.

For room temperature liquids, the inlet system was modified to replace the supply tank with a glass vessel shown in Figure 3b. The liquid was introduced by syringe into the vessel while a dry nitrogen flow was purging the vessel. The vessel was then connected to the inlet system and the vessel inserted into a liquid nitrogen bath to freeze the liquid. The entire vessel and lines were then evacuated. After evacuation, the vessel was removed from the liquid nitrogen bath and warmed to room temperature thereby releasing the trapped gases in the liquid. This process of freezing, evacuating, and thawing was repeated at least three times or until all evidence of trapped gases (bubbles) was gone. The liquid was then allowed to warm to room temperature (~20°C) before each experiment. If the vapor pressure was insufficient to cause the required attenuation of the beam, the liquid vessel was gently warmed with a water bath to increase the vapor pressure enough to give the required attenuation.

B. Materials.

The model peptide used for all of the experiments was physalaemin obtained from Sigma Chemical Company. Physalaemin is an undecapeptide that has well known fragmentation patterns.[19,20]

The peptide was dissolved in methanol and mixed with the FAB matrix at 20 mg/ml concentration. The matrix used was "magic bullet", a 3:1 mixture of dithiothreitol:dithioerythritol, which is a commonly used matrix for FABMS of peptides.[21]

III. Results.

A. Cross Sections.

The initial efforts were directed toward setting the optimal parent ion attenuation with the target gases. As reported by Curtis et al. for this instrument, the daughter fragment intensities tended to be maximized at 70 to 90 per cent attenuation of the parent ion.[21] The maxima depended somewhat on the target gas used, however. Since helium was the target gas most used, other target gases were evaluated against it, with 90% used as the attenuation setting for all experiments. Since an accurate gauge of the pressure in the cell itself did not exist, I determined if at a beam attenuation of 90% whether the number of target gas molecules in the collision cell (N) changed when target gases were changed.

Because the collision process follows Beer's Law, the product of the collisional cross section, σ, and number density, N, of the target gas at 90% attenuation with a collision cell path length, l, of 2 cm, is found by:

$$0.1I_o = I_o\exp(-\sigma N l) \quad (34)$$

or $$\ln(0.1) = -\sigma N(2.0\ \text{cm}) \quad (35)$$

and then $$\sigma N = 1.15\ \text{cm}^{-1}. \quad (36)$$

So therefore, the number of target gas molecules in the collision cell, N, is dependent on the collisional cross section of the parent ion and target gas used. The collisional cross section must then be determined.

The collisional event can be approximated by a collision between two spheres of radii, r_{pi} and r_t. The maximum distance between centers of mass when they can just collide is equal to the sum of their radii, $r_{pi} + r_t$. The maximum collisional cross section is then the circle described by:

$$\sigma = \pi(r_{pi} + r_t)^2 \quad (37)$$

Since the parent ion used is large (>1000 daltons), then r_{pi} is much greater than r_t in all cases. Because of this, σ can be approximated as:

$$\sigma \approx \pi r_{pi}^2 \quad (38)$$

Knowing this, if the attenuation is constant then N is a constant also. In this manner, the number density will be held constant (to a first approximation) during all experiments. Therefore, the average number of collisions experienced by the parent ion will also be the same under all target gas

compositions at 90% attenuation of the parent ion beam.

B. Physalaemin Fragmentation.

In looking for a model peptide with mass greater than 1000, physalaemin seemed to be a good choice. It has the structure, pGlu-Ala-Asp-Pro-Asn-Lys-Phe-Tyr-Gly-Leu-Met-NH_2 (Scheme I) and it generates a molecular ion in FABMS of 1265.6. It is readily available from commercial sources in pure form and its fragmentation pattern has been fairly well documented.[19,20] The low resolution FAB spectrum is shown in Figure 4. The molecular ion at *m/z* 1265 gives a strong signal but fragmentation, especially to give higher mass fragments, is weak or absent. High resolution FABMS measurements were performed on several selected peaks and the data are given in Table II. The high resolution measurements were compared against the literature fragmentation assignments[19,20] and the errors from calculated masses of those ions are also in Table II.

Four representative peaks were chosen from the FABMS/MS spectrum (Figure 5): one low mass fragment, two middle mass fragments, and one high mass fragment. The purpose being to quantify effects of target gases on the relative intensities of these representative peaks.

The first peak chosen, *m/z* 1232, has apparently not been discussed in the literature. Because it showed good intensity in the MS/MS spectrum, I attempted to determine the fragmentation pattern that creates it. As shown in Scheme I, I propose a

fragmentation scheme that comes from stepwise loss of NH_3 from the M+H peak to give *m/z* 1248.57 and then loss of CH_4 to give *m/z* 1232.54. The *m/z* 1248.57 peak has been reported by Boyd, et al.[20] as resulting from loss of NH_3 from the N-terminal methionine of physalaemin. Loss of 16 mu (CH_4) from the side chain of methionine would give the *m/z* 1232 peak. The stepwise loss of 16 mass units is seen in the spectrum of methionine (Figure 6), where it can be seen that the loss of 16 mu (CH_4) from the *m/z* 133 ion gives a weak peak at *m/z* 117. Although loss of CH_4 is apparent in methionine, other locations in the physalaemin ion can lose methane, so labeling studies would have to be performed to prove the origin of the neutral loss. Even so, this type of fragmentation is reportedly due to lower energy processes so this peak's intensity was monitored in subsequent experiments.

Another peak whose fragmentation source was questionable was the *m/z* 84 peak. Biemann, et al.,[19] stated that it is due to lysine and/or pyroglutamic acid. No data were given to support this so experiments were conducted to attempt to confirm the source and the mechanism of formation of this fragment. FABMS/MS on the *m/z* 968.5 peak (which Boyd assigned to y'' cleavage[22] between Pro and Asp) and also the *m/z* 741.4 peak (which he assigned to z cleavage between Lys and Asn) showed (Figure 7) that the *m/z* 84 peak was derived from the *m/z* 741 peak and was present in the MS/MS spectrum of the *m/z* 968 peak (Figure 8). This supports the Lys site as the source of the peak, with the nitrogen of the fragment coming from the amide group between Lys

and Phe.

The next step was to run MS/MS on the *m/z* 784 peak which has been assigned as b cleavage between Tyr and Phe.[19,20] This spectrum confirmed that one source of the *m/z* 84 peak is this section of the molecule. The mechanism of the fragmentation is still unknown but Biemann has stated[23] that these low-mass fragments from the interior of a peptide have the general structure, $[H_2N{=}CHR]^+$, where R in this case would be C_3H_3O. Another possible fragmentation pathway to this daughter ion is a-type fragmentation from pGlu. This fragmentation is observed in other pGlu C-terminal peptides but usually in low intensity. Unfortunately, physalaemin does not have normal FABMS daughter ions that contain this section of the molecule which would allow the determination of the likelihood of this pathway for *m/z* 84. The normal FABMS spectrum has too much chemical noise below *m/z* 100 to recognize this daughter and to determine if it is a significant fragmentation in normal FABMS. Due to this inability to rule out pGlu as a source, one must assume that some intensity comes from this pathway. However, one can also assume that any variation in this peak's intensity is primarily due to increased likelihood of internal fragmentation, which should have a higher activation energy barrier. For this reason, its intensity was also monitored during subsequent experiments.

To complete the observations, two more peaks were observed in the middle of the MS/MS spectrum. The first choice was the *m/z* 323 peak, which was assigned to an internal fragment containing Pro-Asn-Lys which then loses NH_3 (probably from

Asn).[19] Finally, the *m/z* 784 peak which involves simply b cleavage between Tyr and Phe.

C. Target Gas Effects.

Using helium as benchmark since it is most widely used,[2,3] a number of gases were employed to test the effects of different gases on the intensities of the four peaks that were previously selected from the MS/MS spectrum of physalaemin. The gases were common ones (H_2, He, N_2, CH_4, Ar) plus a few more exotic gases to include polyatomics (D_2, Ne, CHF_2CH_3). The spectra were collected in raw form and the individual peaks measured by hand, because the smoothing and centroiding routine normally employed caused unacceptable errors in peak height in some instances. An example of the raw data is shown in Figure 9.

The data showed a general trend that supports the previous work,[24] in that the more massive the target gas, the more intense the lower mass fragment peaks. The higher mass peaks decreased in intensity with increasing target masses. The data are summarized in Table III.

The data are shown with relative intensity (daughter ion intensity/parent ion intensity x100) plotted versus target gas mass in Figures 10-13, for fragment ions *m/z* 1232, 784, 323, and 84, respectively.

D. Target Vapor Effects.

The next series of experiments used low boiling liquids as target "vapors". The vapor pressures of benzene and acetonitrile were not high enough at moderate temperatures (25-30°C) to be useful. Acetonitrile tended to condense at the inlet capillary to the collision cell and was very slow to pump away. Low boiling (<50°C) liquids of low molecular weight, (<100 amu), were next chosen as target vapors. Another criterion was the average atomic weight based on Derrick's statistical approach to the impulsive theory. Since physalaemin has an average atomic weight of 7.273 mu, furan and acetaldehyde, which have average atomic masses close to that number, were chosen. The data are summarized in Table III and included in the graphs in Figures 10-13.

IV. Discussion.

A. Efficiency of Energy Transfer.

The energy transfer efficiency of a given target gas and parent ion combination is the amount of energy that is internalized by the parent ion during a given collisional event. One could argue that the total amount of fragmentation, i.e., the sum of all daughter ion intensities would be a measure of this energy transfer efficiency. This does not account, however, for

changes in competing processes such as scattering or neutralization reactions as one changes targets. A different measure of energy transfer efficiency must be found. In searching for this measure, one can assume that low mass ions formed from internal fragments would be formed by fragmentation pathways with higher activation energies than by simple cleavages between amino acid residues or by losses of simple neutrals such as H_2O, NH_3, and CH_4. Using this reasoning, the activation energies of the various fragments studied here would be generally $E_{1232} \approx E_{784} < E_{323} < E_{84}$. The trend observed from the data is that the high mass daughter ion, *m/z* 1232 , decreased in intensity while the *m/z* 84 peak increased in intensity when the target gas mass was increased. Plots of the relative intensities of tges peaks to one another as a function of target gas mass are shown at Figures 15-20. As can be seen, the *m/z* 84 peak appears to increase at the expense of the *m/z* 784 and 323 peaks. The other graphs show two regions; a quick rise to a maximum then a nearly linear decrease. The exception to this is the *m/z* 84 versus 1232 graph, which has more scatter.

The implication of this type of analysis of the data is that the fragmentation observed generates *m/z* 84 daughter ions by sequential unimolecular decay from both the *m/z* 784 peaks and the *m/z* 323 peaks. Figure 14 shows a reaction diagram that explains this process.

In this sequential reaction, only when P^+ has enough internal energy can it overcome the activation energy barrier to decompose forming daughter ion D_1. If enough internal energy is

left, it can further overcome the next energy barrier to form daughter D_2, and so on until the pathway ends. For daughters to be detected by the second mass spectrometer, they must be formed in the collision cell (transit time ca. 0.8 μsec for *m/z* 1265.6) and must have a lifetime greater than or equal to the transit time to the detector (ca. 60 μsec for *m/z* 1232).

Using this argument, the data can be explained by the energy transferred by collision increasing with the mass of the target gas. This energy transfer will have a statistical distribution of energies that will cause population of each step in the decomposition pathway. The population of each daughter ion is determined by the total energy required by the route to that daughter ion and the energy transferred in a given collision. Since the energy transferred is a statistical distribution for a given target gas, the intensities will maximize for daughter ions that have total activation energies less than or equal to the average energy transferred to the parent ion by that target gas. Since the only variable in these experiments is the difference in target gases, the mechanism of energy transfer must then be related to target mass.

B. Energy Transfer Mechanism.

The relative intensities of the peaks as a function of mass (or average mass) may be a method of looking at the energy transfer efficiency. If the daughter ion intensities are directly proportional to the amount of energy transferred to the

parent ion in a collision and since the amount of energy is constant in these experiments (omitting vibrational and rotational energies), then the efficiency of that energy transfer is the only difference that will account for the trends. The efficiency of energy transfer is probably a function of the mechanism of energy transfer. The electron excitation mechanism that is generally accepted is only dependent on the velocity of the parent ion and the adiabatic criterion, a_e. This value a_e is an interaction distance in effect and has values that are on the order of 2×10^{-8}cm for helium and 7×10^{-8} cm for methane. The Massey theory predicts a slowly decreasing probability of energy transfer as the mass of the target increases. This is consistent with data for the *m/z* 1232 and 784 daughter ions. The *m/z* 323 and 84 daughter ion data show maxima that are not predicted by this theory. The impulsive theory does explain these data and predicts a maximum when the statistical (average) mass of the target gas is the same as the statistical (average) mass of the parent ion. In this case the maximum is predicted at 7.27 amu and this is approximately where the data reach a maximum for the *m/z* 84 peak (Figure 13). If one accepts the impulsive theory then the shape of the plots of *m/z* 1232 and 784 peaks as a function of target mass can be explained by statistical arguments. The formation of *m/z* 1232 and 784 may be intermediate states in the formation of lower mass daughters. These intermediate states then become depleted as increasing energy predicted by the impulse theory causes the decomposition to proceed to lower mass daughter ions. This has been observed by

the relationship of *m/z* 784 to 84 previously discussed. The *m/z* 1232 ion probably has many possible fragmentation pathways and the relationship to one subsequent daughter may be undeterminable, as is demonstrated by the *m/z* 84 vs. 1232 data.

V. Conclusions.

The data suggest that increasing the mass of the target increases the energy transferred to the vibrational modes of the parent ion (physalaemin), which is exhibited by the increased low mass daughter ion intensities at the expense of high mass daughter ion intensities. The electronic excitation mechanism predicts that no increase of fragmentation should occur and in fact predicts that the overall energy transferred should decrease. Although the overall intensity of the daughter ions does decrease as the target mass increases this can be accounted for by the increasing effects of the scattering and charge neutralization occurring at the expense of collisional activation intensities.

These experiments have shown a strong argument for the impulsive method of energy transfer for collisionally activated dissociation of higher mass peptides (>1000). This may mean that both electronic and vibrational excitation occur in a collisional event, but the relative contribution shows an inverse relationship with parent ion mass for electronic excitation and a direct relationship to vibrational excitation of the impulsive type. The data further suggest that the maximum energy transfer

occurs when the target gas average atomic mass is the same as or similar to that of the parent ion.

From a practical standpoint, the data suggest that optimization of collision activation efficiency for a given parent ion would involve matching the target gas average mass as closely as possible to the average mass of the parent ion.

The natural conclusion from this line of reasoning is that the parent ion is its own best target gas for collisional activation. This is not feasible in the classical manner of introduction of target gases or vapor, but one can get close as demonstrated with the vapors of furan and acetaldehyde. A program was developed (Figure 21) to assist the scientist in tailoring a target gas/vapor to the parent ion of interest. In truly practical terms this would be worth the effort for large (>2000 daltons), hard-to-fragment molecular ions.

More work should be performed to study the present conditions using the full velocity of the ions. The expected result is that higher energies would be internalized by the parent ion in each case versus the floated cell experiments. The dissociation reactions then should proceed further to low mass daughter ions and, therefore, the ratio of low mass intensities to high mass intensities with a given target gas should be greater than with the parent ion beam slowed to half its original velocity. The overall intensities may be unpredictable since the VG 70 SE-4F spectrometer was optimized by the manufacture for floating cell operation.

This research generates a proposal for an interesting

theoretical instrument that would use an opposing beam of identical parent ions at a 180° incident angle to provide a means of ideally matching the parent ion with the target. It would be, in effect, its own target gas. Colliding the beams along a single axis in an activation region would result in scattering but would also maximize the amount of energy transferred to both molecules. To borrow an analogy from the real world, this would be similar to a head-on collision on the freeway. The activation region where the beams collide could be the source area for the analysis of daughter ions by accelerating the ions at a right angle to the collisional axis into another mass spectrometer. Since the acceleration grid near the activation region would probably need to be pulsed so as not to affect the beams except when collecting a packet of daughter ions, a time-of-flight mass spectrometer would be the best analyzer for the resulting daughter ions. This postulated instrument could look something like Figure 22.

The advantages could be in that the two parent ion beams could be selected by any of the current beam-type mass/charge analyzers. The parent ion intensity would be double that of a single beam instrument and, since no target gas is used, differential pumping would be eliminated in the activation region.

In practical use however, many technical problems would have to be overcome, not the least of which would be achieving matched monoenergetic, tightly focused, colinear beams. Since perfect focusing, colinearity, and energy matching is doubtful, high

scattering losses would be the result. In addition, the ion optics of the right angle mass spectrometer would have to compensate for the residual velocities of the ions perpendicular to the axis of that spectrometer.

Another more promising approach to the problem of increasing the activation energy in tandem mass spectrometry is electron-induced dissociation (EID). The use of electrons has greater potential for electronically exciting the parent ion than either collision with a target gas or photon absorption. The technical problems involved in deaccelerating the parent ion beam to increase the cross section for interaction (collision) with the electron beam, while maintaining sensitivity and transmission, is difficult but not insurmountable. The location and operation of the electron filament in or close to the beam path is perhaps a more difficult task but this has already be done to some extent.[14] Further research on the feasibility of this activation mechanism with sector instruments seems appropiate.

Tables

Table I

Calculated Average Masses of Various Types of Compounds

Compound	Avg Mass	Compound	Avg Mass
H_2	1.01	Acetic Acid	5.50
H_2O	6.00	Alanine	6.85
CO_2	14.66	Glucose	7.51
CH_4	3.21	Benzene	6.51
MeOH	5.34	Butanol	4.94
Ethane	3.76	CH_2Cl_2	16.98

Table II

Comparision of High Resolution Data for Physalaemin

m/z (nominal)	Observed Value	Error (mmu)
784	784.3616	1.4
741	741.3883	0.1
323	323.1720	-0.1

Table III

Ion Intensities (Percentages of Molecular Ions) with Various Common Gases

			Fragment (*m/z*)			
Target	Mass	Avg Atomic Mass	84	323	784	1232
H_2	2.016	1.008	1.76	1.91	6.56	0.68
D_2	4.032	2.016	2.91	5.67	9.40	3.94
He	4.002	4.003	1.78	1.73	3.36	2.66
CH_4	16.037	3.20	16.87	4.60	3.40	2.03
N_2	28.014	14.007	13.47	4.09	3.21	2.9
Ne	20.184	20.184	9.04	2.57	2.53	1.68
Ar	39.947	39.947	6.22	1.33	1.45	1.30
$C_4H_4F_2$	80.080	7.27	9.1	0.61	0.91	1.74
Furan	68.05	7.56	13.80	1.52	1.74	2.28
CH_3CHO	44.050	6.29	11.92	1.87	2.28	2.59

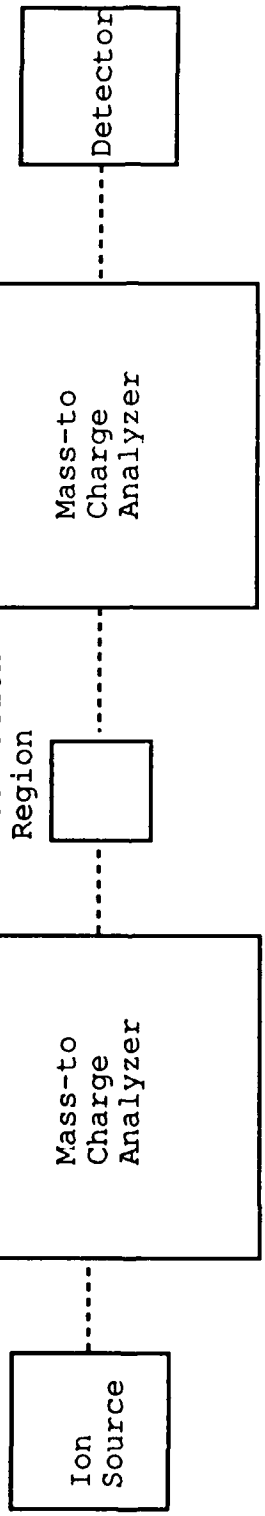

Figure 1. Black Box Diagram of Tandem Mass spectometer

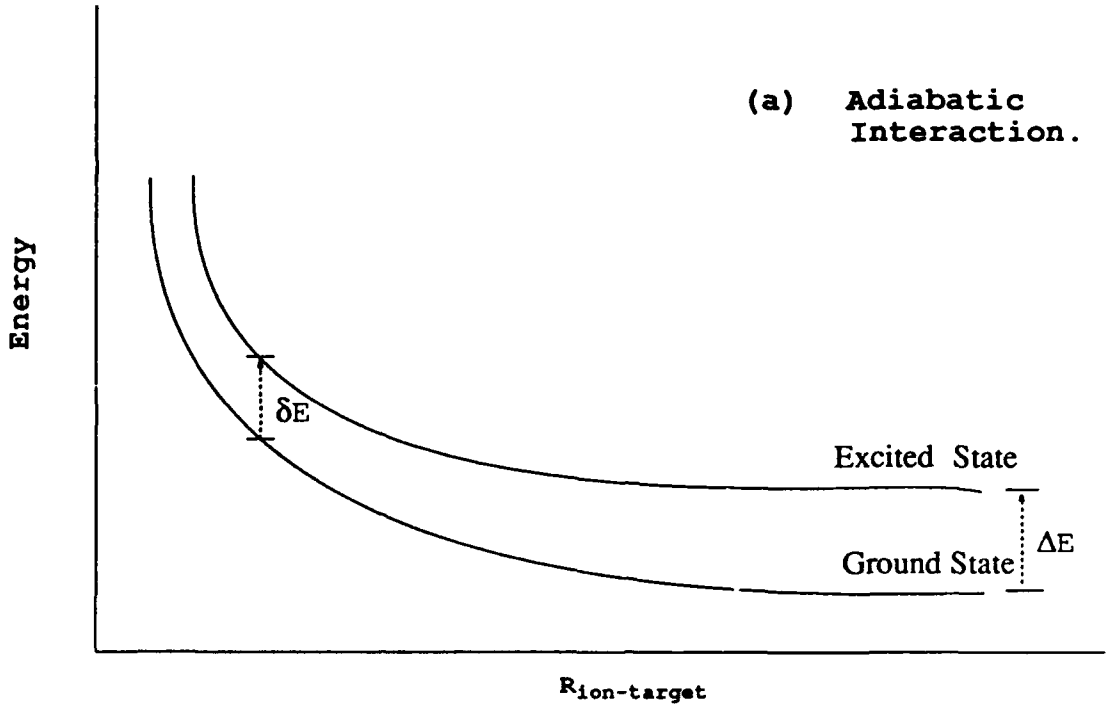

Part (a): Electronic energy level diagram during adiabatic interaction.

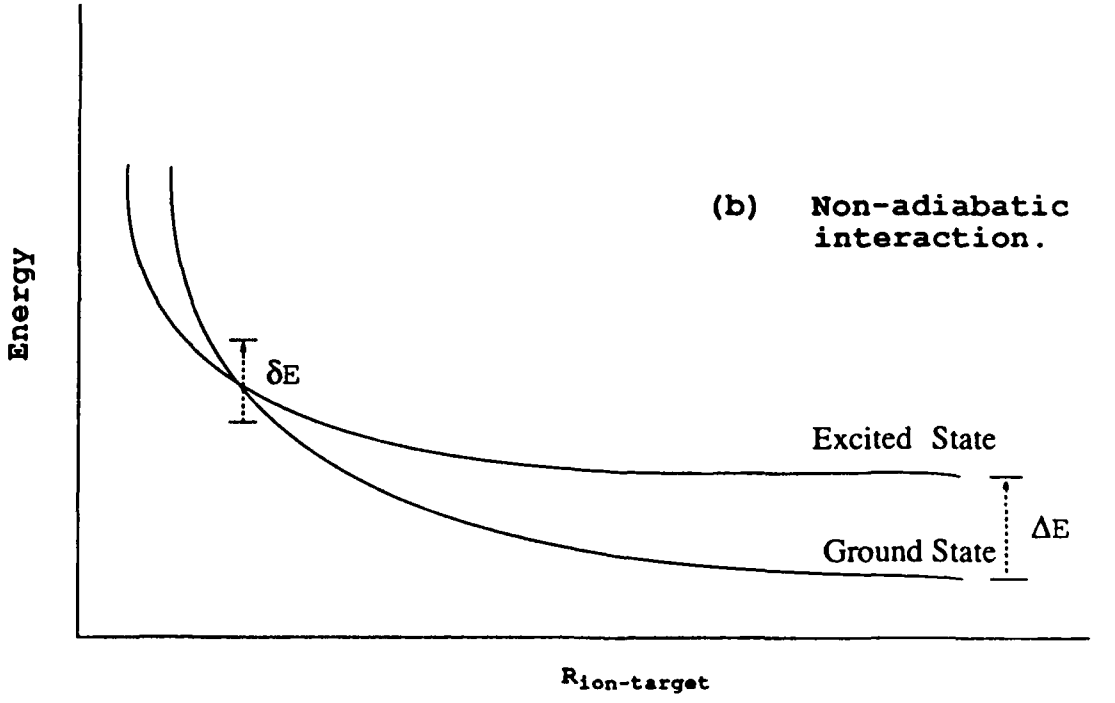

Figure 2. Electronic energy level diagrams of adiabatic and non-adiabatic interactions.

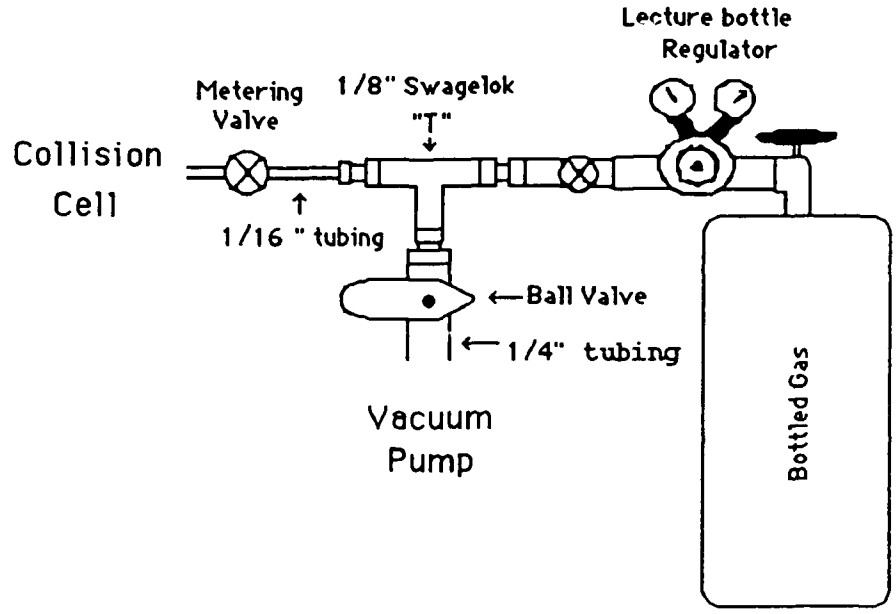

Figure 3a. Target Gas Inlet System

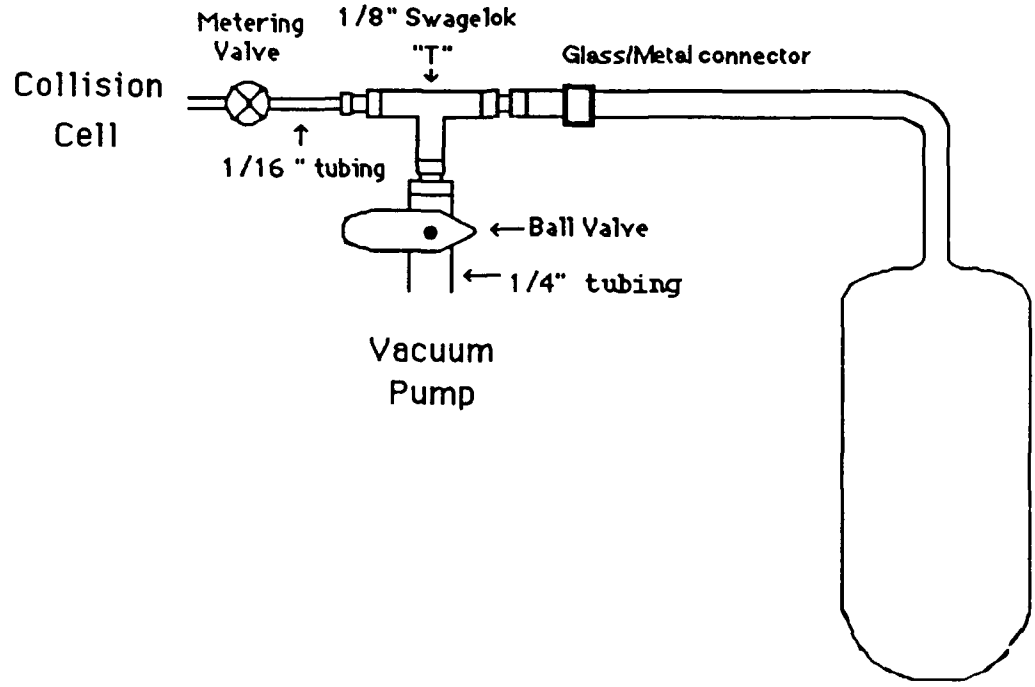

Figure 3b. Vapor Inlet System

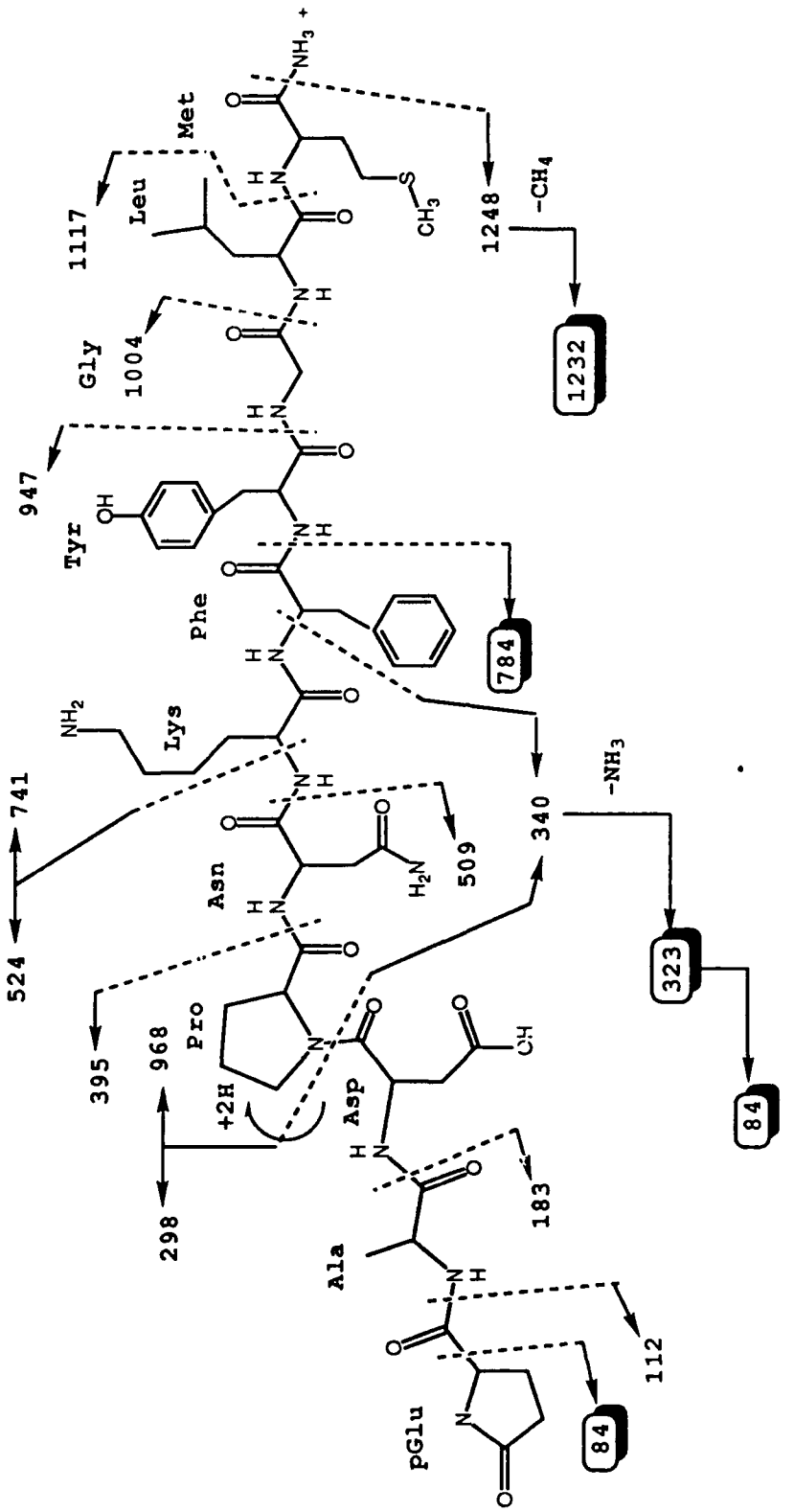

Scheme I. Fragmentation of Physalaemin.

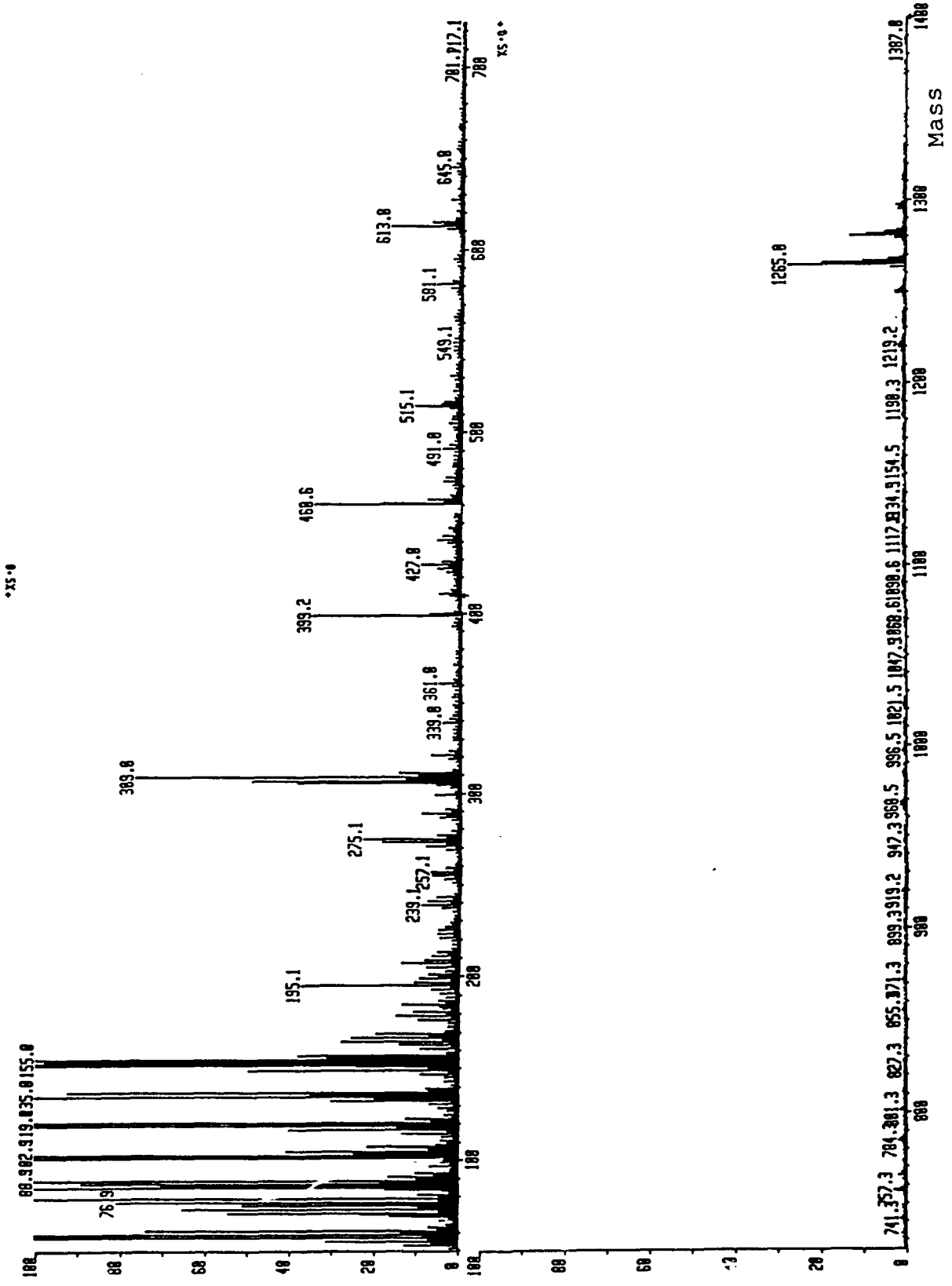

Figure 4. Low Resolution FAB Spectrum of Physalaemin In Magic Bullet

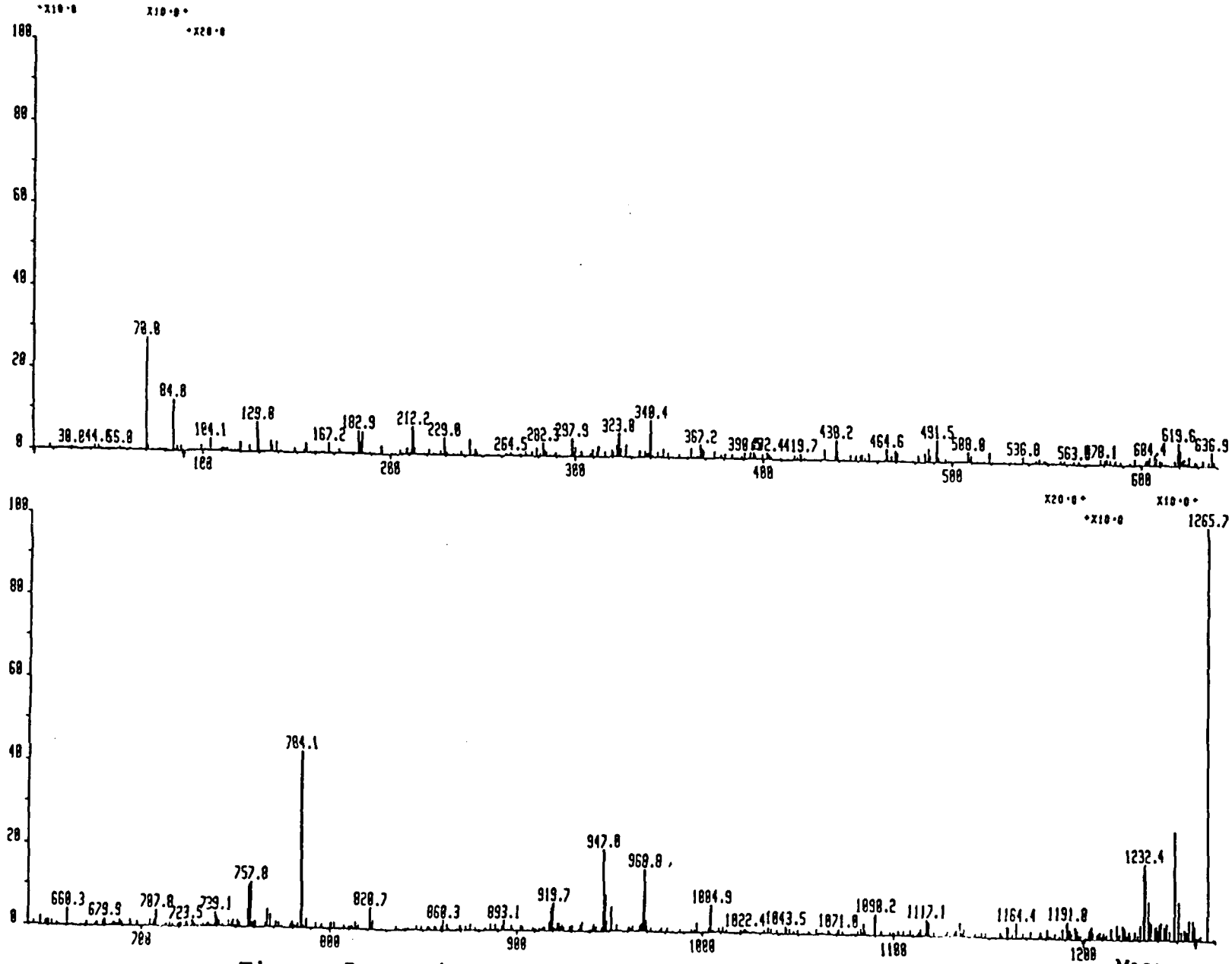

Figure 5. MS/MS Spectrum of Physalaemin Molecular Ion *(m/z 1265.56)*

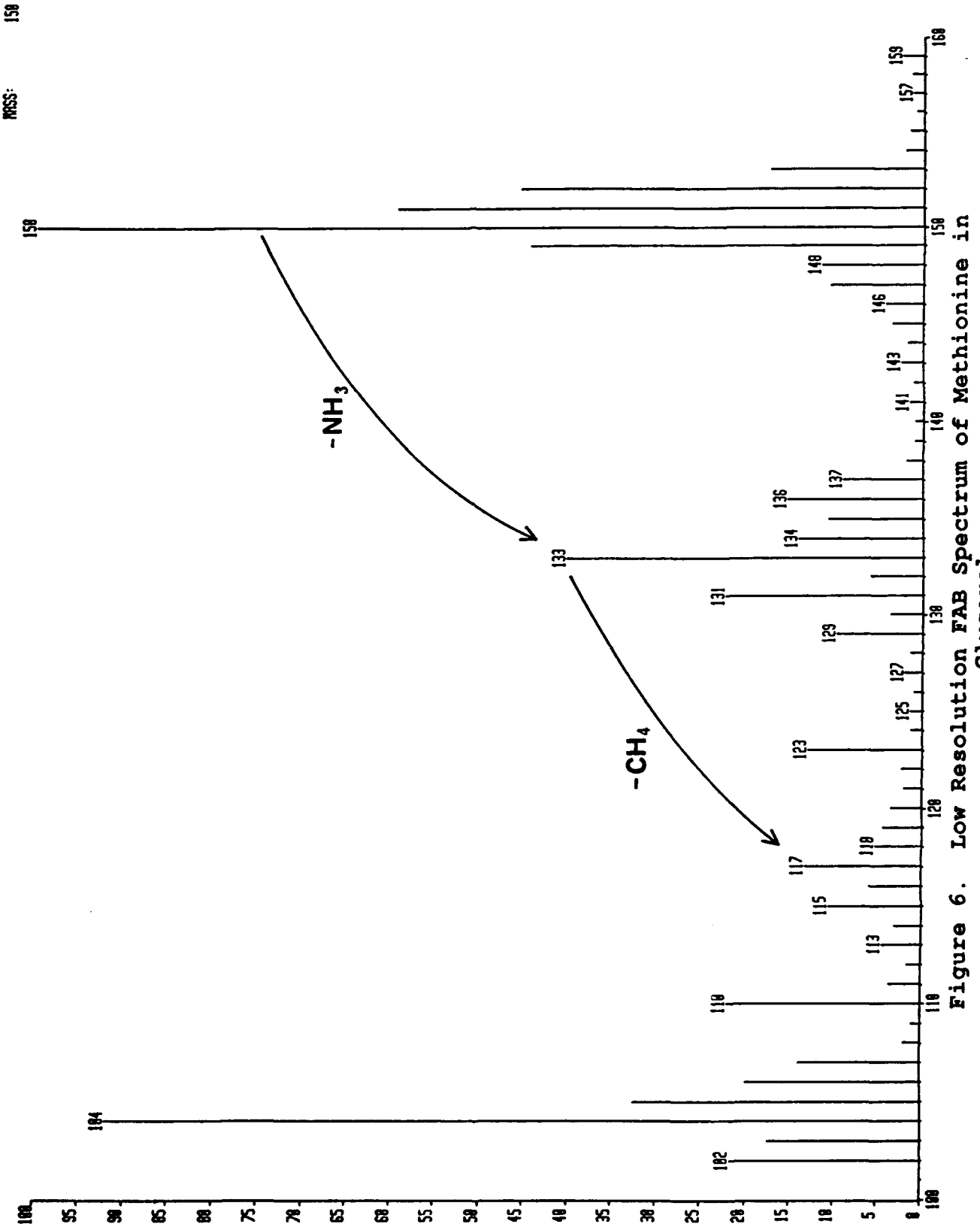

Figure 6. Low Resolution FAB Spectrum of Methionine in Glycerol

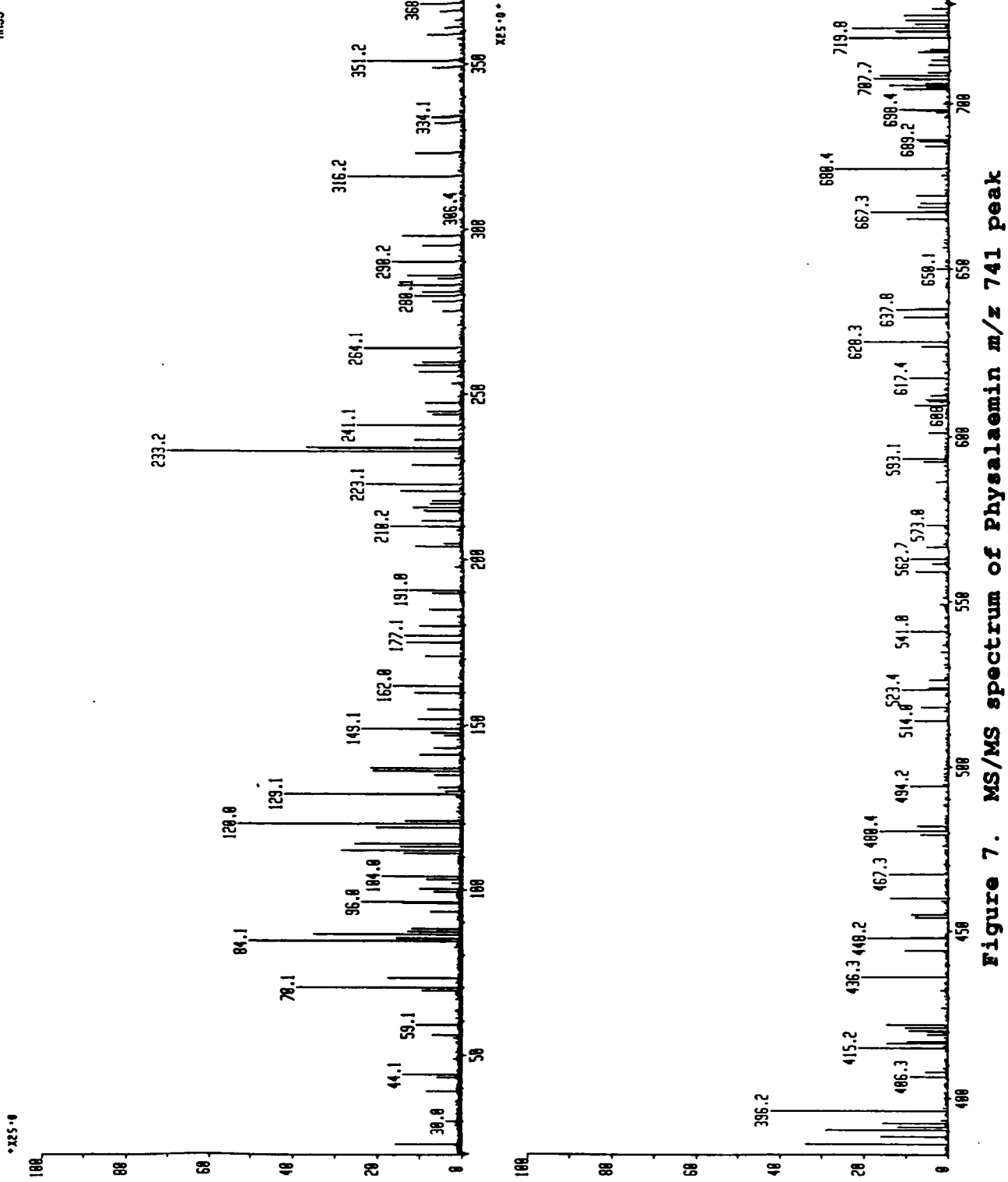

Figure 7. MS/MS spectrum of Physalaemin m/z 741 peak

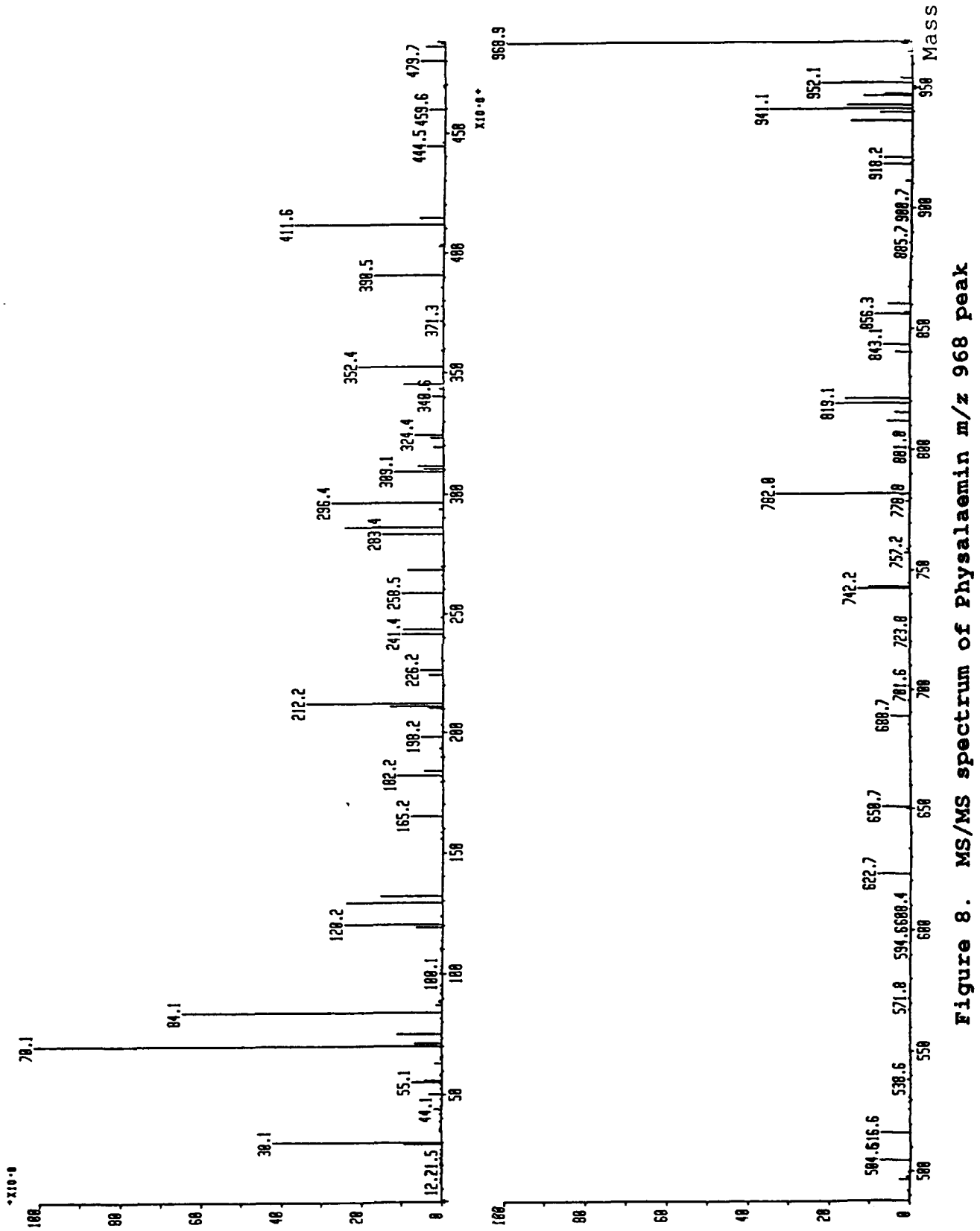

Figure 8. MS/MS spectrum of Physalaemin m/z 968 peak

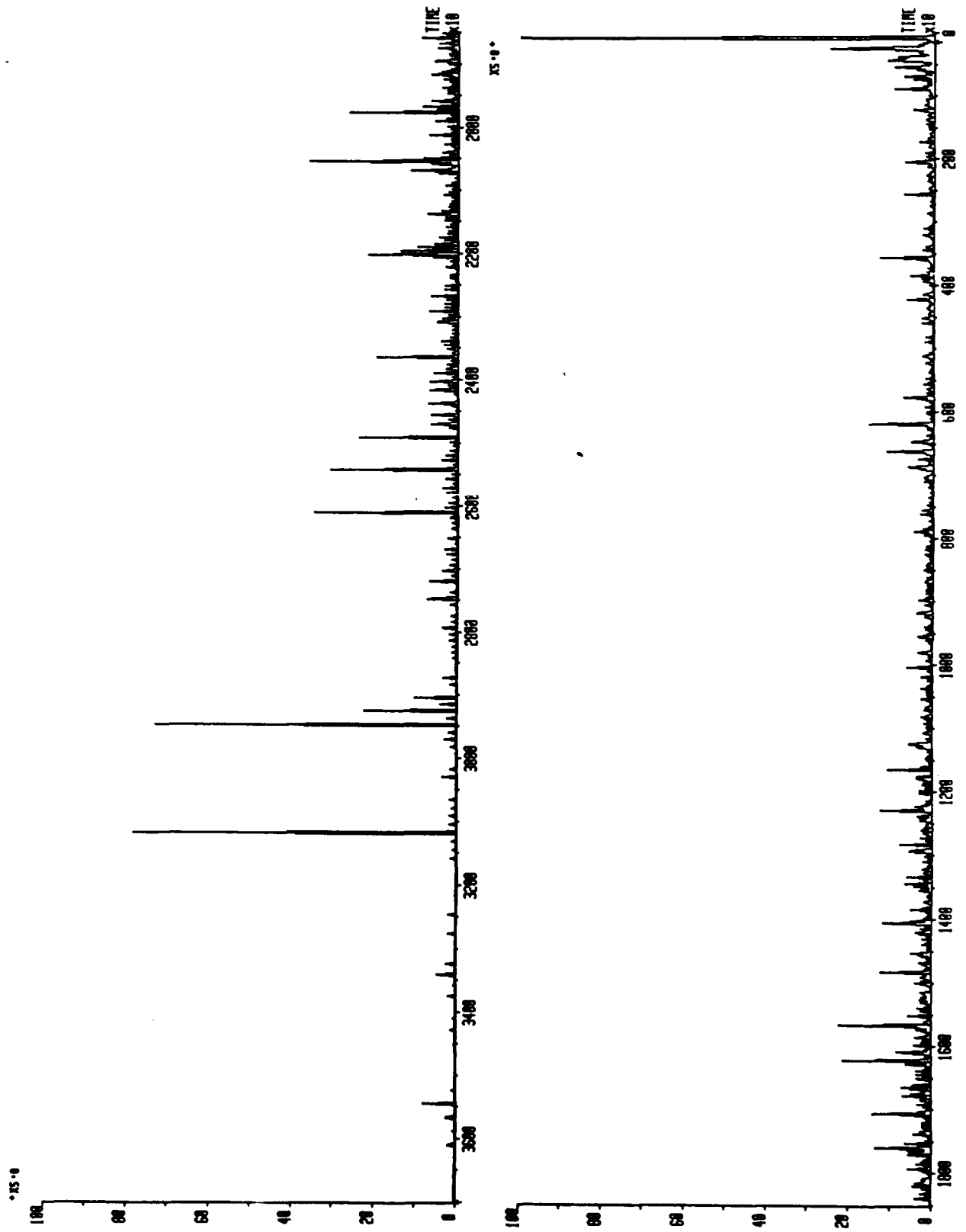

Figure 9. Example of Raw Continuum Data.

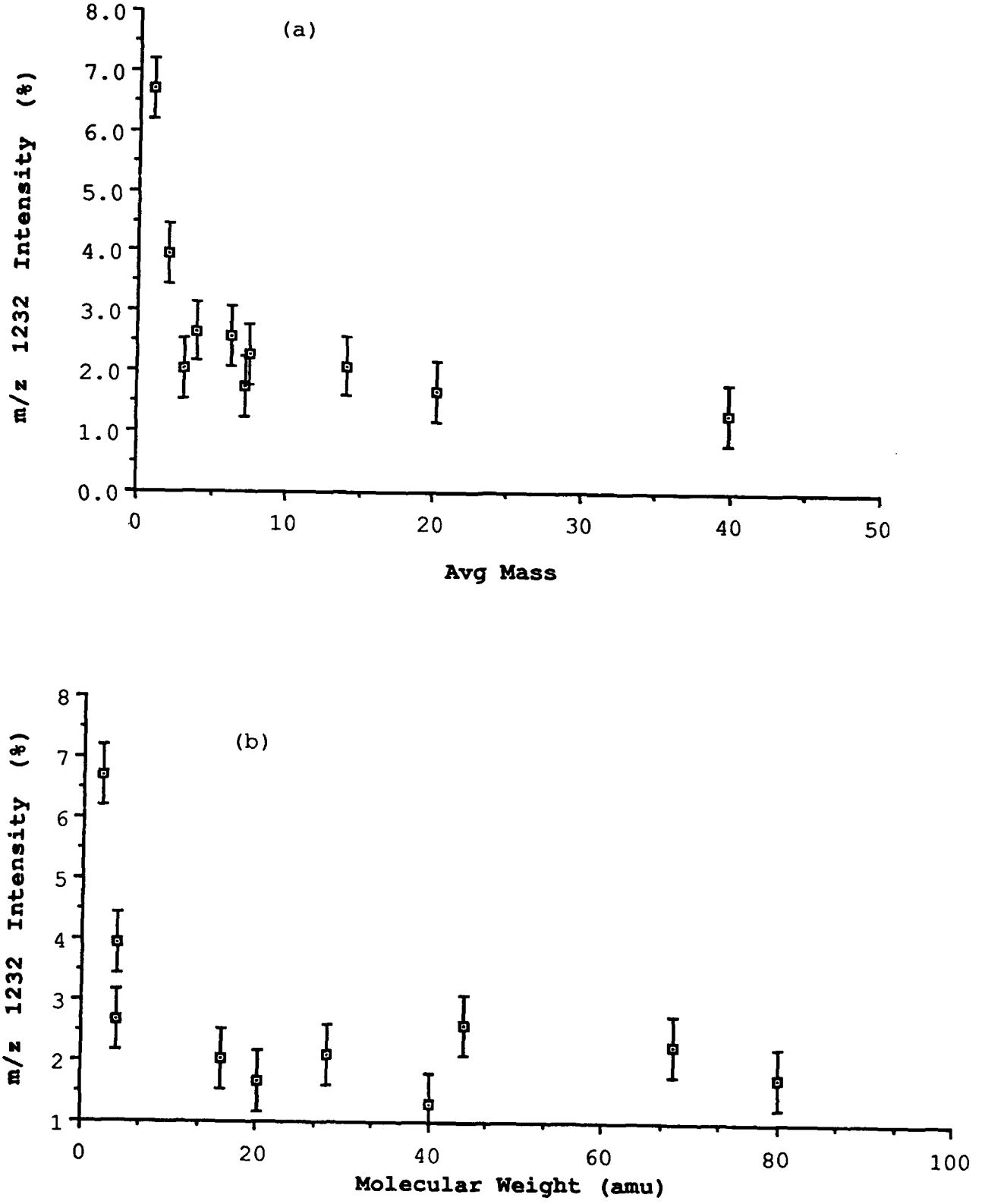

Figure 10. m/z 1232 daughter ion intensity vs average mass (a) and molecular weight (b) of target gas.

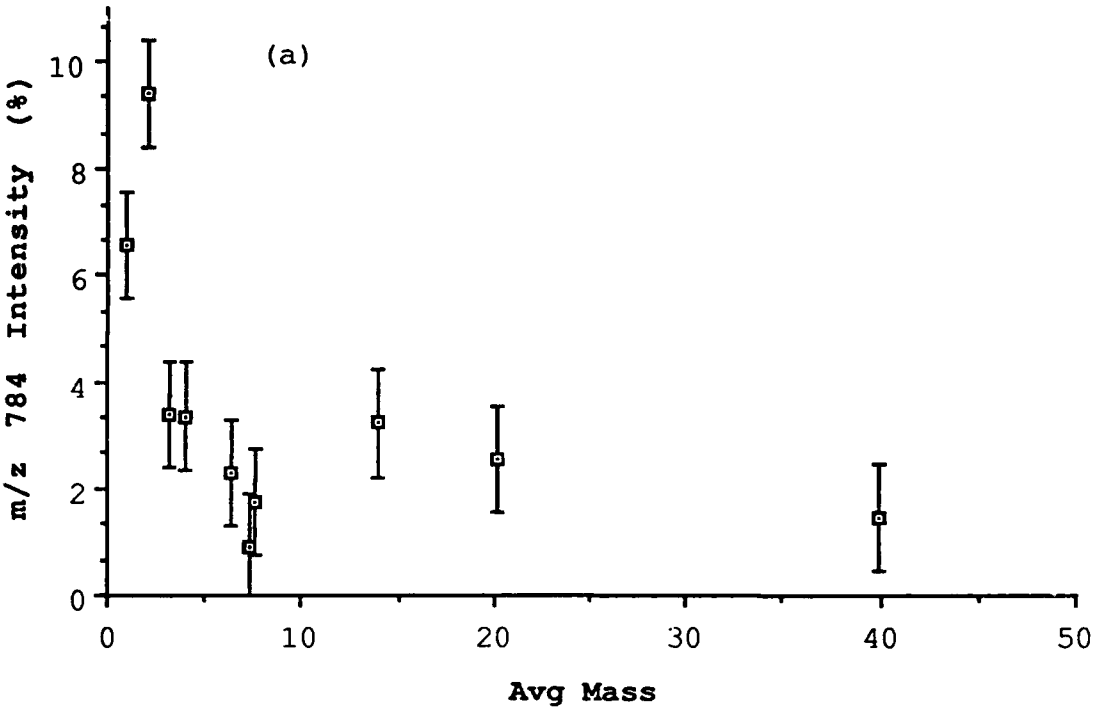

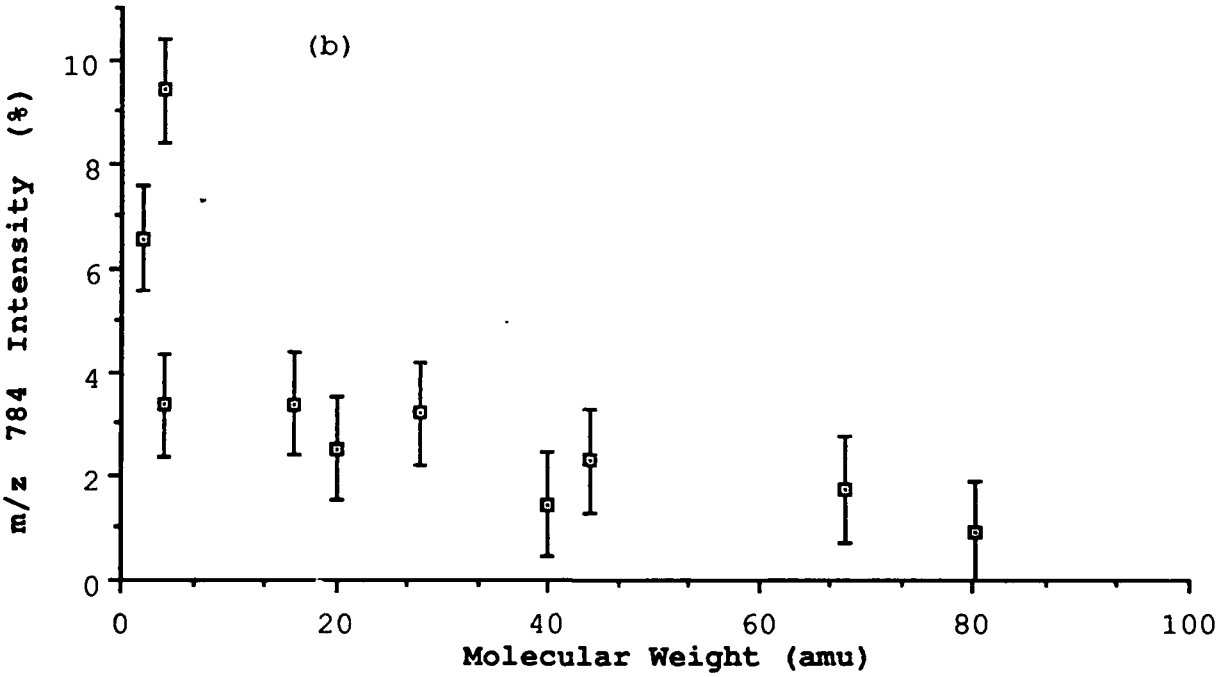

Figure 11. m/z 784 daughter ion intensity vs average mass (a) and molecular weight (b) of target gas.

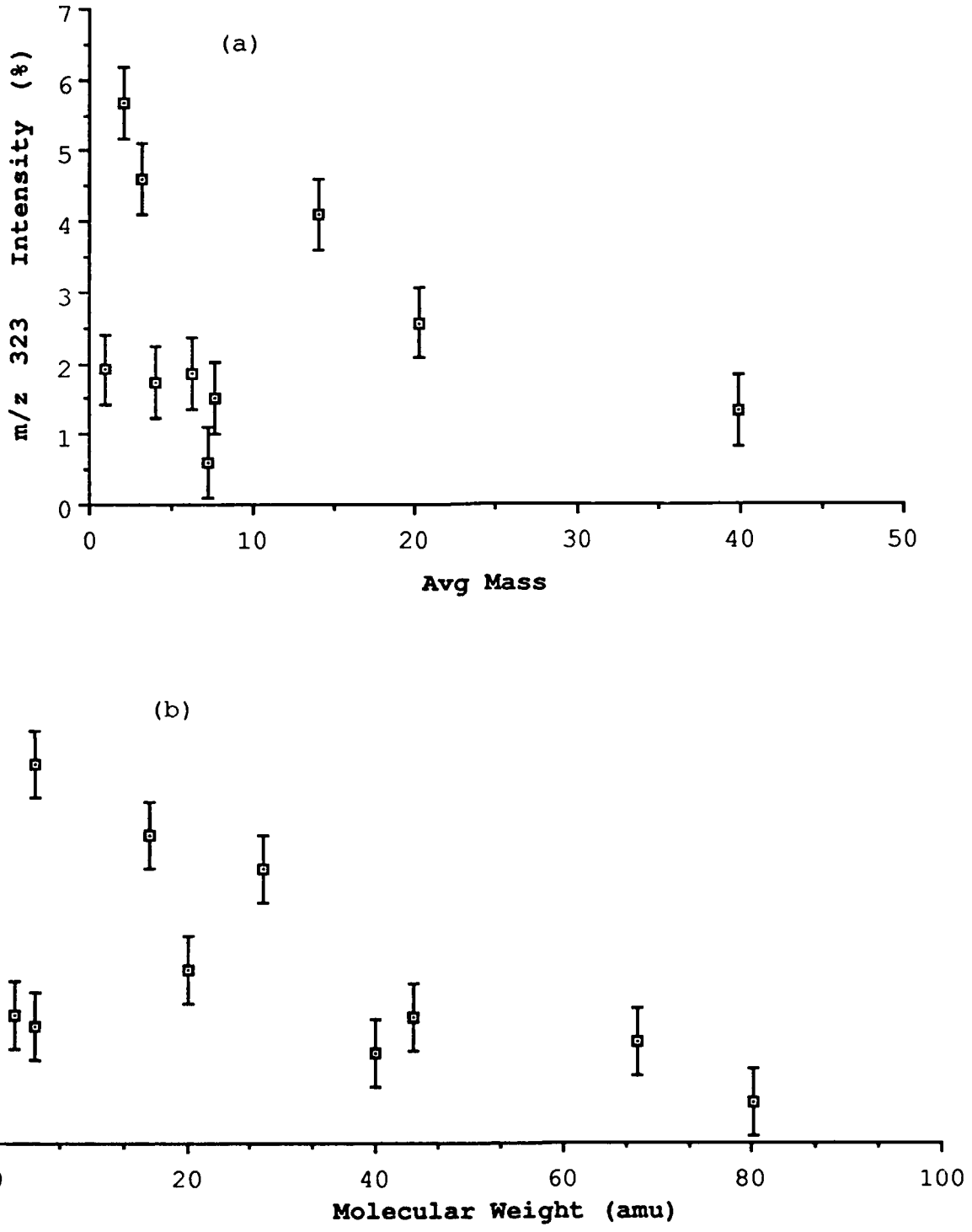

Figure 12. m/z 323 daughter ion intensity vs average mass (a) and molecular weight (b) of target gas.

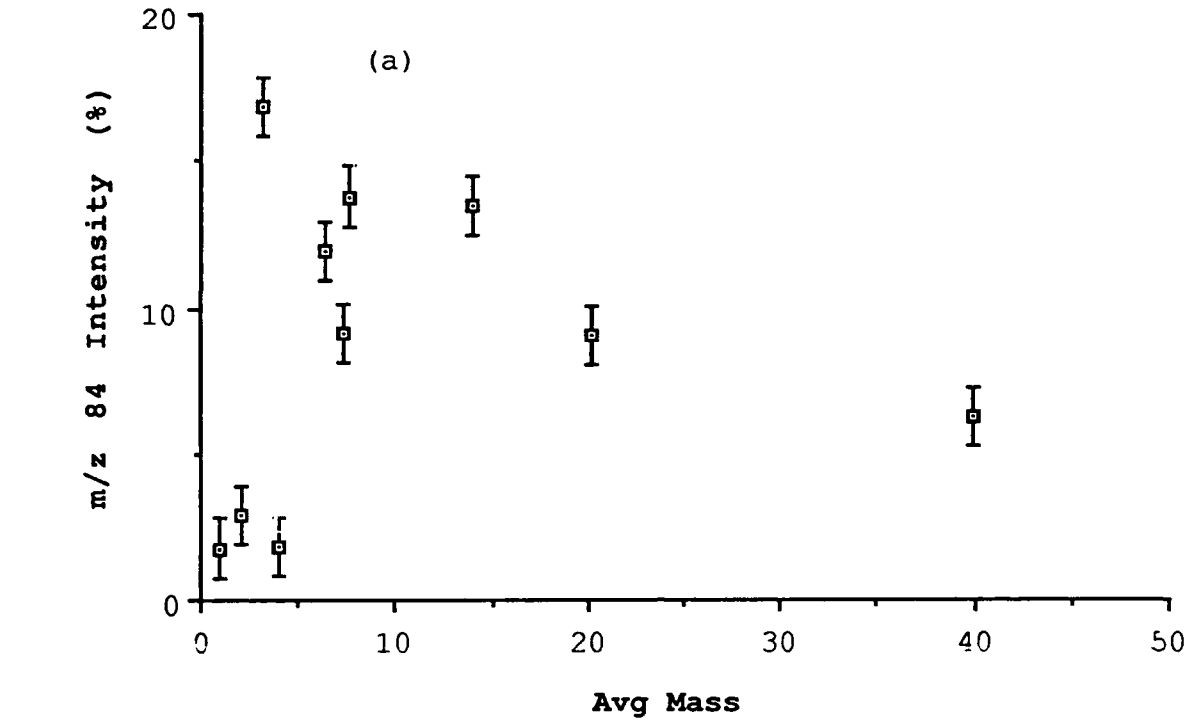

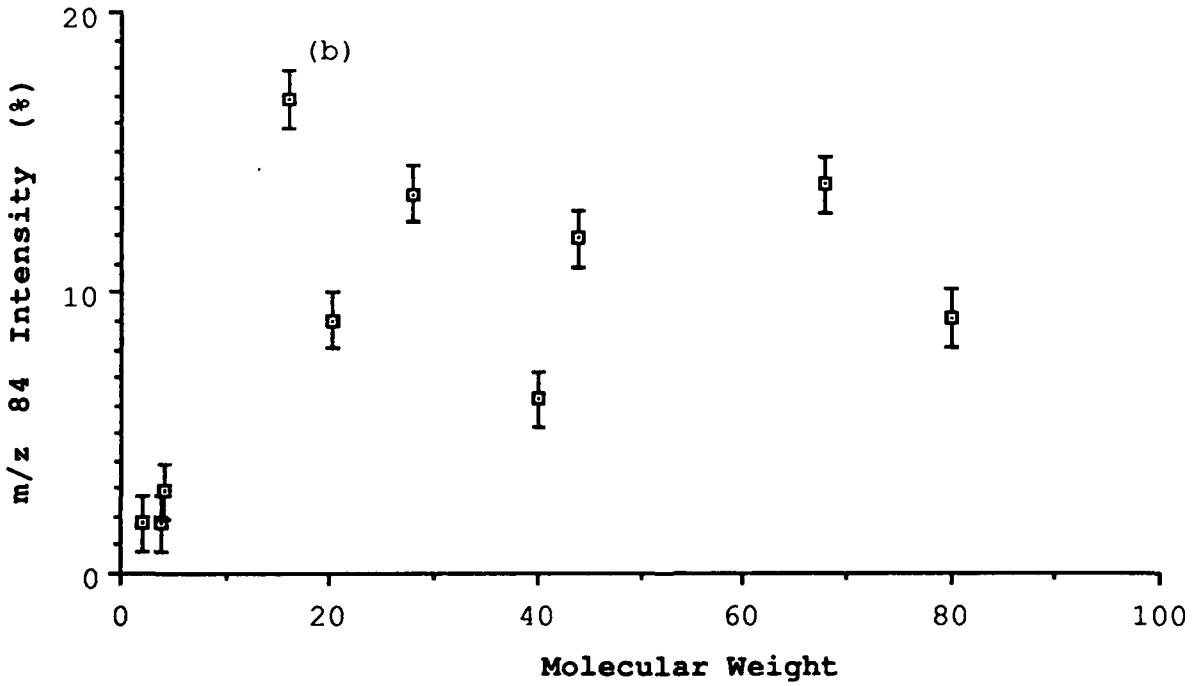

Figure 13. m/z 84 daughter ion intensity vs average mass (a) and molecular weight (b) of target gas.

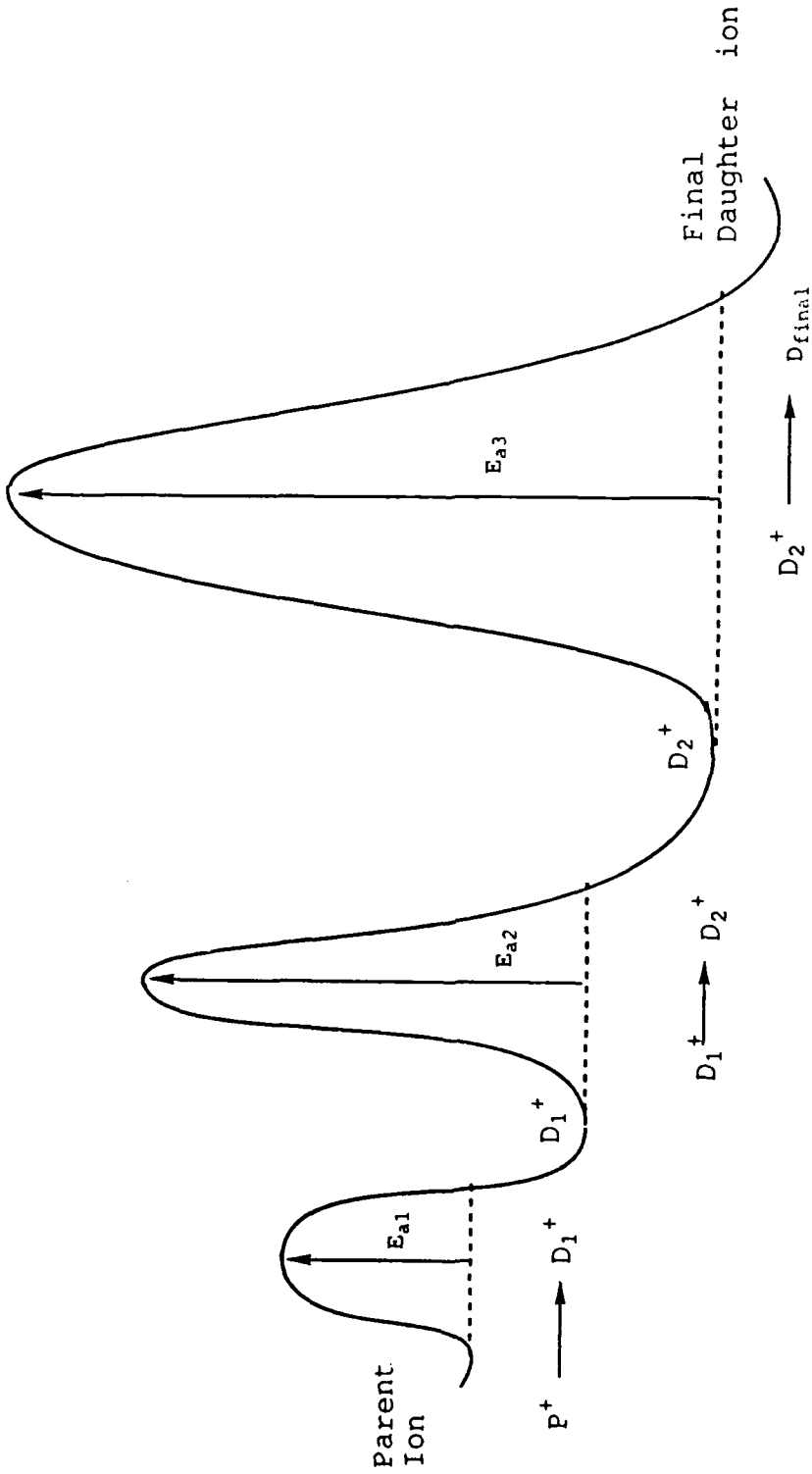

Figure 14. Example of Sequential Reaction Diagram

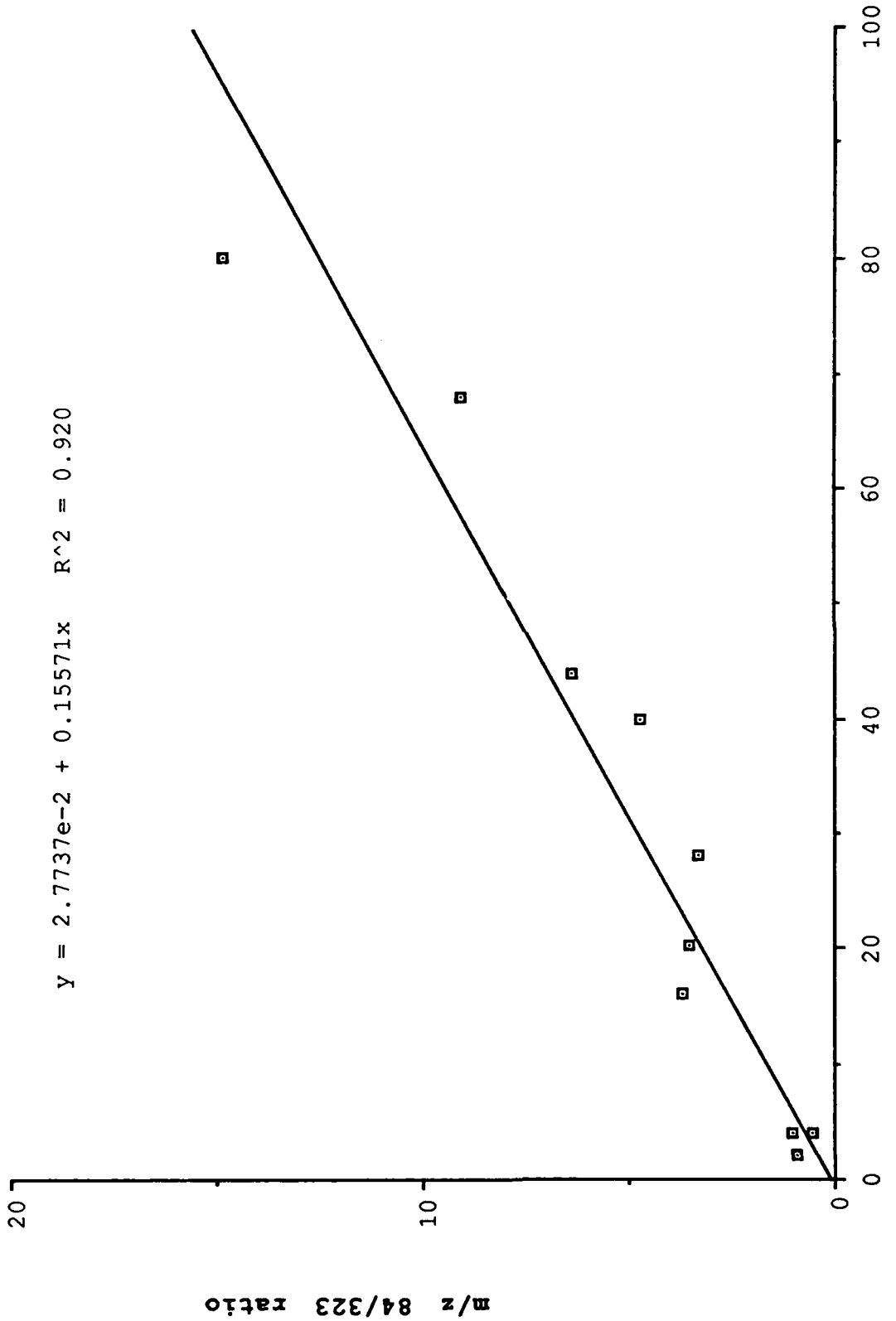

Figure 15. Ratio of 84/323 Relative Intensities vs Target Gas Mass.

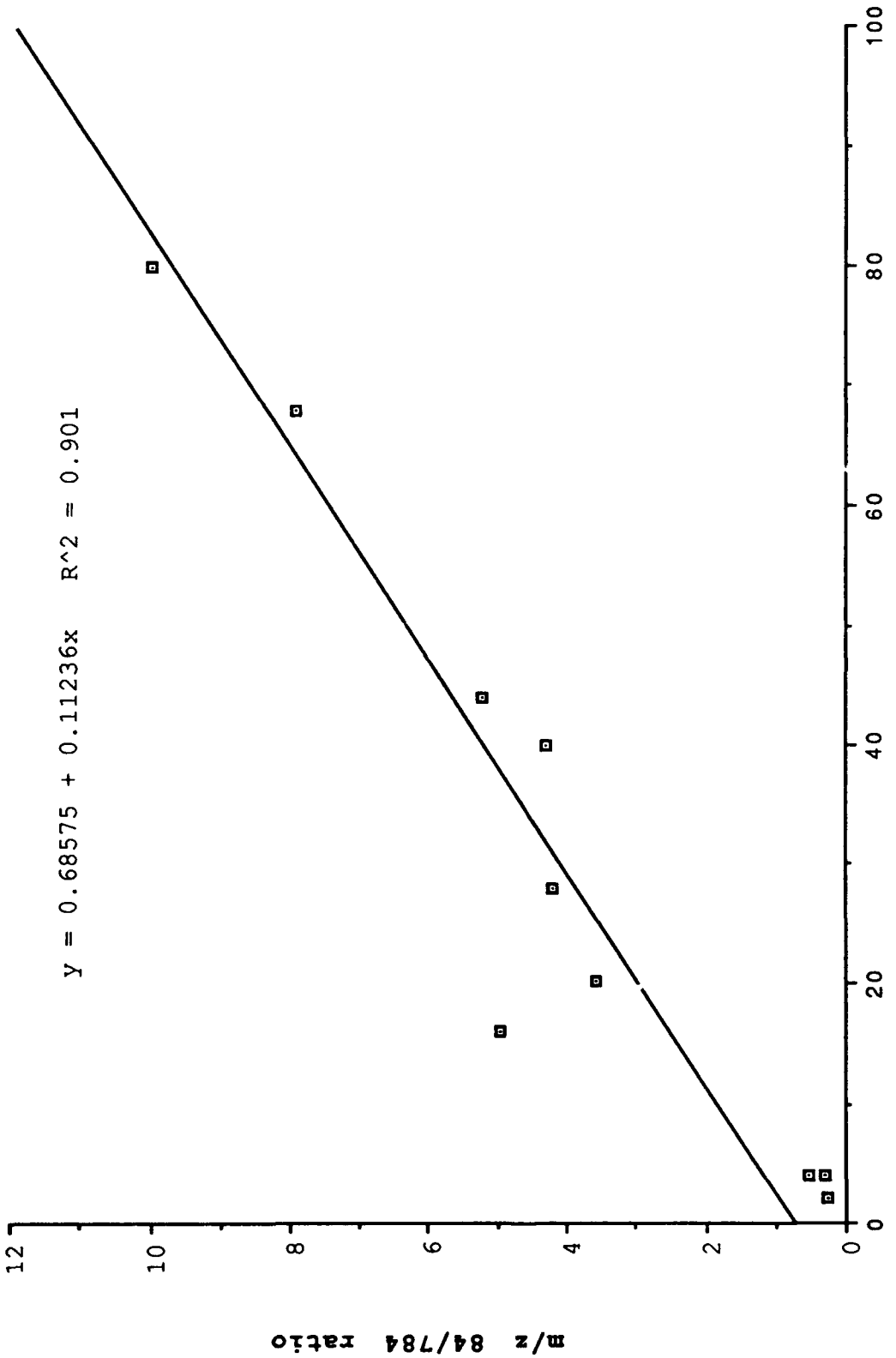

Figure 16. Ratio of m/z 84/784 Relative Intensities vs Target Gas Mass.

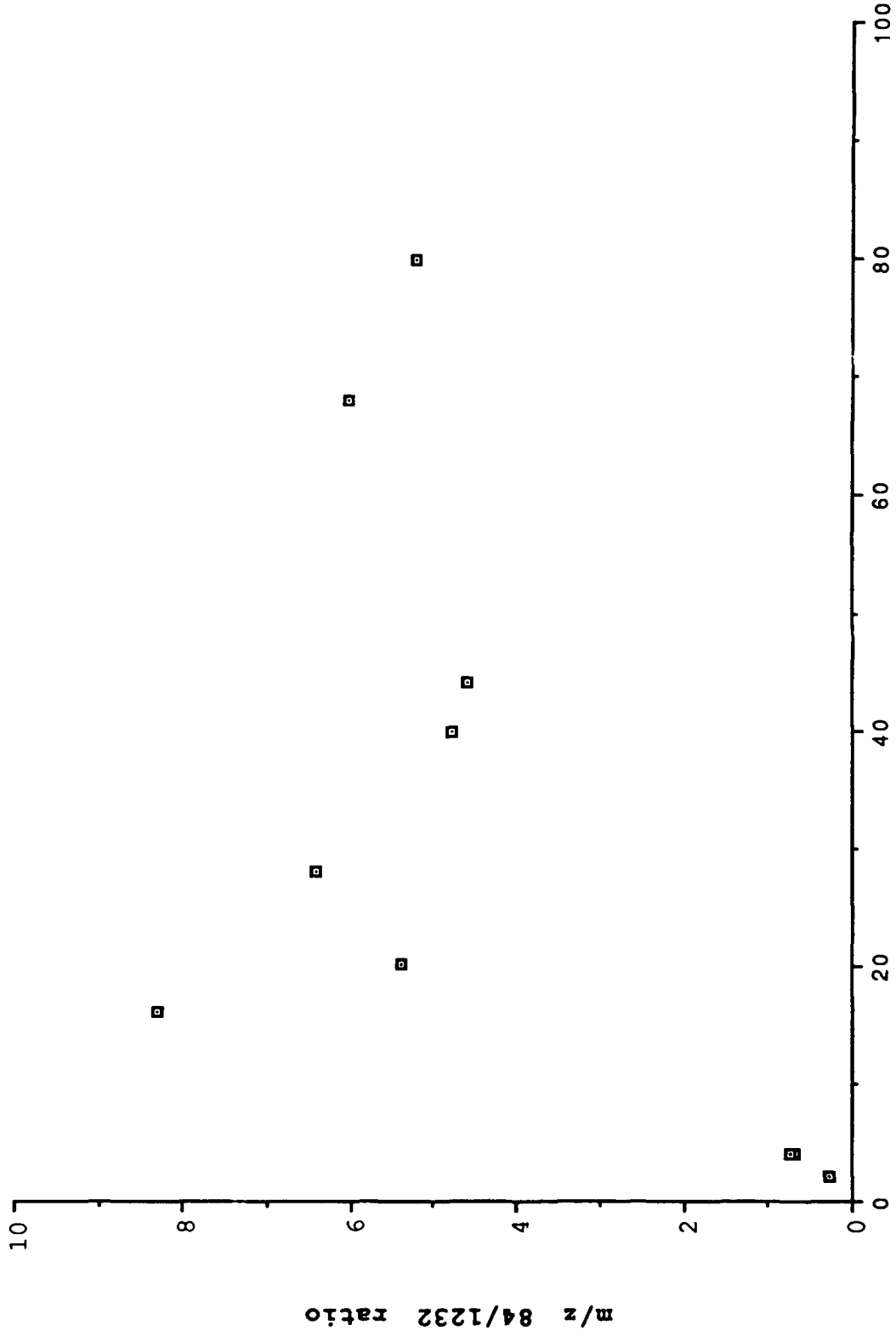

Figure 17. Ratio of m/z 84/1232 Relative Intensities vs Target Gas Mass.

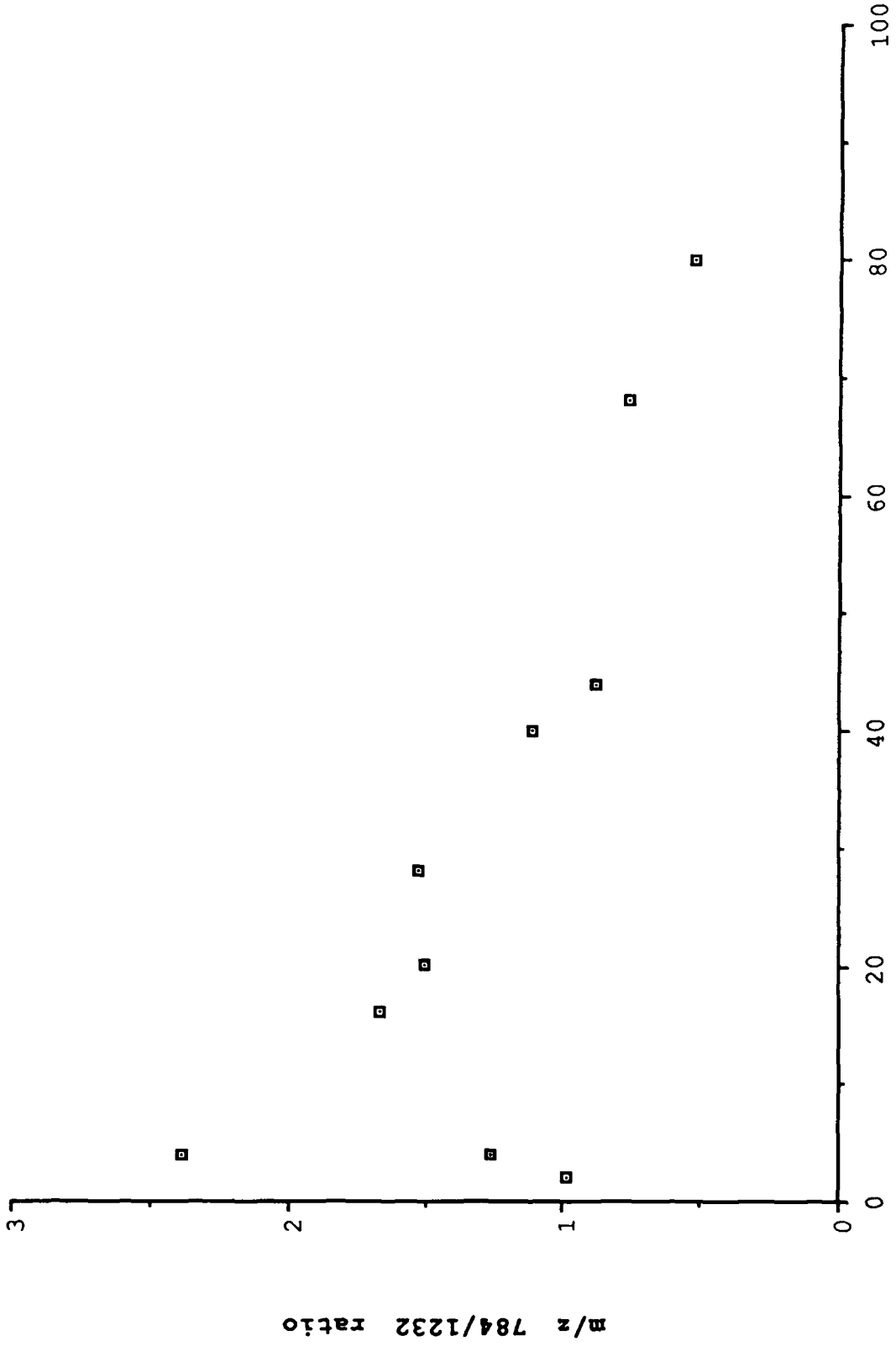

Figure 18. Ratio of m/z 784/1232 Relative Intensities vs Target Gas Mass.

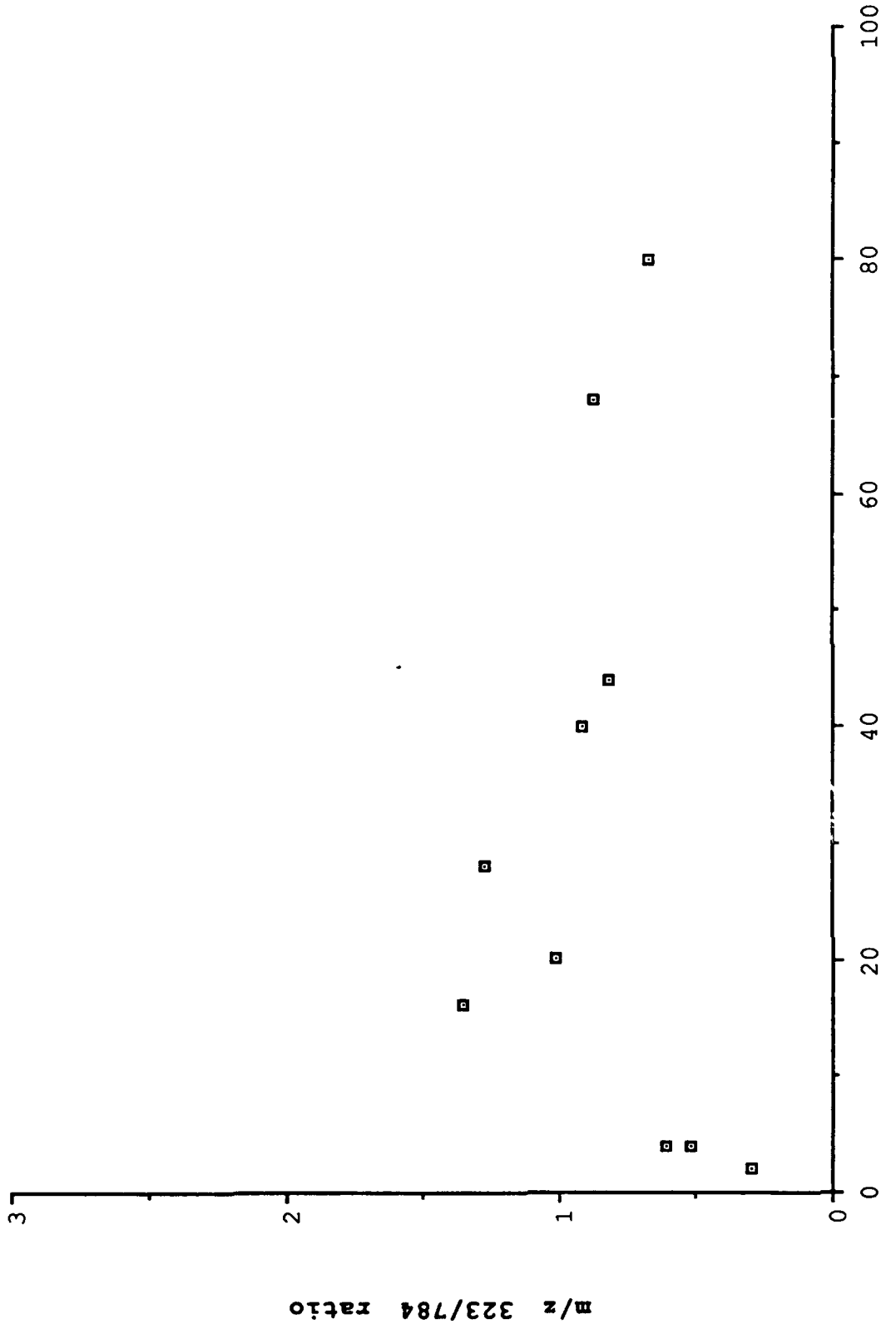

Figure 19. Ratio of m/z 323/784 Relative Intensities vs Target Gas Mass.

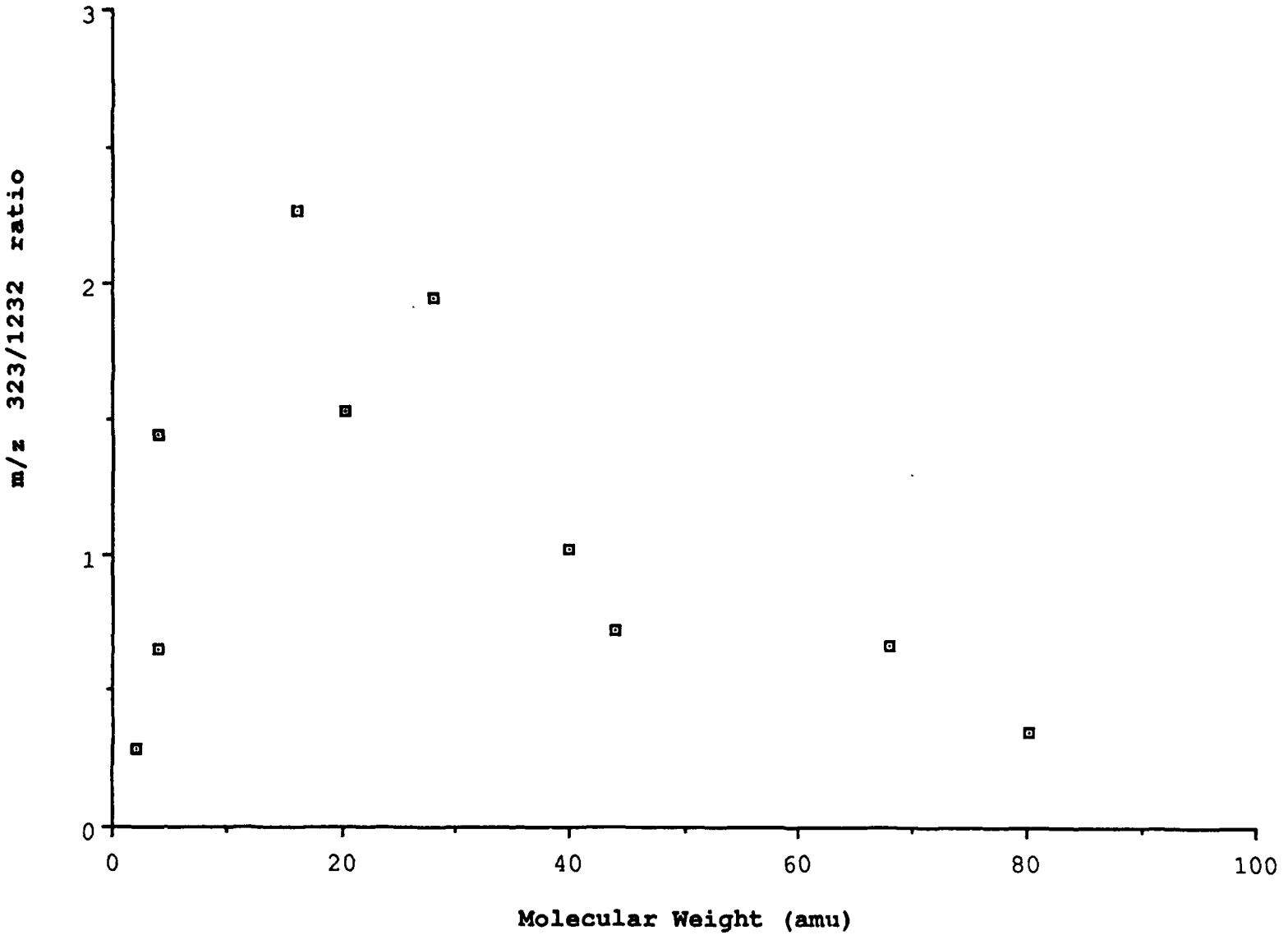

Figure 20. Ratio of 323/1232 Relative Intensities vs Target Gas Mass.

```
100 REM:  This is a simple basic program designed to
110 REM:  calculate all the mathmatically possible
120 REM:  TARGET GASES with an average atomic weight in the
130 REM:  usual peptide range given at line 370.  Only
140 REM:  compounds with C, H, N, O, S, and F are
150 REM:  computed.  Expansion of this program is easily
160 REM:  done by replacing the range endpoints with
170 REM:  variables and inserting an input line for the
180 REM:  endpoints at the beginning.  Also, the compound
190 REM:  composition can be adapted by adding more atom
200 REM:  FOR,NEXT loops and changing the maximum for each.
210 REM:  It does some checks to eliminate impossible
220 REM:  compounds but it doesn't catch all of them.
230  FOR F=0 TO 3
240  FOR S=0 TO 3
250  FOR O=0 TO 3
260  FOR N=0 TO 3
270  FOR H=0 TO 10
280  FOR C=1 TO 4
290  X=12*C+14*N+H+16*O+32*S+19*F
300  Y=C+H+N+O+S+F
310  Z=X/Y
320  W=C-H/2+N/2+1
330  Q=2*C+2
340  IF Y-C>Q THEN 380
350  IF W>4 THEN 380
360  IF X>100 THEN 380
370  IF Z>6.8 AND Z< 8.0 THEN LPRINT
      "C"C"H"H"N"N"O"O"S"S"F"F, "Avg ="Z, "DB ="W
380  NEXT H
390  NEXT N
400  NEXT O
410  NEXT S
420  NEXT F
430  END
```

Figure 21. GW Basic Program for determining possible target gases with the desired average atomic weight.

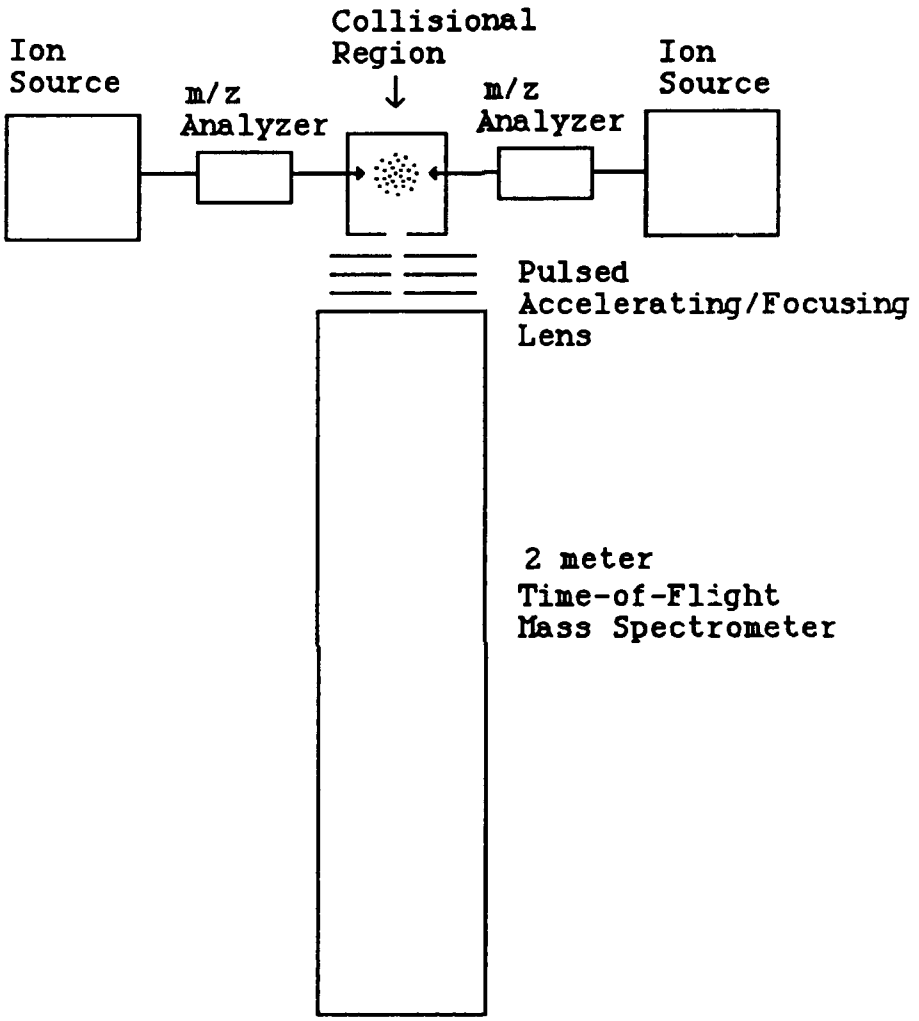

Figure 22. Diagram of Postulated "Double-Beam" Tandem Mass Spectrometer.

References

1. McLafferty, F. W. In *Tandem Mass Spectrometry*; McLafferty, F. W. Ed.; Wiley: New York, 1983; Chapter 1.

2. Bieman, K.; Martin, S.A.; Scoble, H. A.; Johnson, R. S., Papayannopoulos, J. A., Biller, J. E. , and Costello, C. E. In *Mass Spectrometry in the Analysis of Large Molecules*; McNeal, C. J., Ed., Wiley: New York, 1986; pp. 131-149.

3. Busch, K. L; Glishi, G. L.; McLuckey, S. A. *Mass Spectrometry/Mass Spectrometry* VCH: New York, 1988; Chapters 1-3.

4. Robinson, P. J.; Holbrook, K. A. *Unimolecular Reactions*; Wiley-Interscience: New York, 1972; Chapters 2 and 10.

5. Todd, P.J.; McLafferty, F. W In *Tandem Mass Spectrometry*; McLafferty, F. W. ed.; Wiley: New York, 1983; Chapter 7.

6. Jackson, J. D. *Classical Electrodynamics*; Wiley: New York, 1962, Chapter 13.

7. Kim, M. S. and McLafferty, F. W. *J. Am. Chem. Soc.* **1978**, *100*, 3279-3282.

8. Massey, H. S. W. *Rep. Prog Phys.* **1949**, *12*, 248.

9. Freisier, B. C.; Jolly, D. L.; Hamer, N. D.; Nordholm, S.; *Chem. Phys.* **1986**, *106*, 413-425.

10. Uggerud, E.; Derrick, P. J. *Z. Naturforsch* **1989**, *44a*, 245-246.

11. Levsen, K. and Schwartz, H. *Mass Spectrometry Review* **1983**, 2, 77-148.

12. Cody, R. B.; Freiser, B. S. *Anal. Chem.* **1979**, *51*, 547.

13. Freiser, B. S. *Int. J. Mass Spectrom. Ion Phys.* **1978**, *26*, 39.

14. Fedor, D. W.; Cody, R. B.; Burinsky, D. I.; Freiser, B. S.; Cooks, R. G. *Int. J. Mass Spectrom. Ion Proc.* **1979**, *31*, 27.

15. Cody, R. B.; Freiser, B. S. *Anal. Chem.* **1987**, *59*, 1054.

16. Tajima, S.;Tobita, S.; Ogino, K.;Niwa, Y. *Org. Mass Spectrom.* **1986**, *21*, 236.

17. Watson, J. T. *Introduction to Mass Spectrometry*; Raven Press: New York, 1985; Chapter 4.

18. Rinehart, K. L.; Holt, T.G.; Fregeau, N. L.; Staley, A. L.; Thompson, A. G.; Harada, K.-I.; Curtis, J. M.; Rong, L.-S.; Sun F.; Shield, L. S.; Gäde, G.; Grimmelikhuigzen, C. J. P.; Doughty, C. C.; Grimshaw, C. E. In *Biological Mass Spectrometry*, Burlingame, A. L.; McCloskey, J. A., Eds., Elsevier Science: Amsterdam, 1990, p. 233.

19. Sato, K; Asada, T.; Ishihira, M.; Runihiro, F.; Kammei, Y. Kubota, E.; Costello, E. E.; Martin, S. A.; Scoble, H. A.; Biemann, K. *Anal Chem* **1989**, *59*, 1652-1659.

20. Boyd, R. K.; Bott, P. A.; Beynon, J. H.; Harvan, D. J.; Hass, J. R. *Int. J. Mass Spectrom. Ion Proc.* **1985**, *66*, 253-270.

21. Witten, J. L.; Schaffer, M. H.; O'Shea, M.; Cook, J. C.; Hemlin, M. E.; Rinehart, K. L. *Biochem. Biophys. Res. Commun.*, **1984**, *124*, pp 350-358.

22. Roepstorff, P.; and Fohlman, J. *Biomed. Mass Spectrom.* **1984**, *11*, 601.

23. Biemann, K. In *The Proceedings of the Sixth International Conference on Methods in Protein Sequence Analysis;* Walsh, K.A., Ed.; Humana; Clifton, NJ, 1986.

24. Alexander, A.J.; Thibault, P.; Curtis, J. M.; Rinehart, K. L.; *Int. J. Mass Spectrom. Ion Proc.* **1990**, *98*,107-134.